

INFORMATION TO USERS

This manuscript has been reproduced from the microfilm master. UMI films the text directly from the original or copy submitted. Thus, some thesis and dissertation copies are in typewriter face, while others may be from any type of computer printer.

The quality of this reproduction is dependent upon the quality of the copy submitted. Broken or indistinct print, colored or poor quality illustrations and photographs, print bleedthrough, substandard margins, and improper alignment can adversely affect reproduction.

In the unlikely event that the author did not send UMI a complete manuscript and there are missing pages, these will be noted. Also, if unauthorized copyright material had to be removed, a note will indicate the deletion.

Oversize materials (e.g., maps, drawings, charts) are reproduced by sectioning the original, beginning at the upper left-hand corner and continuing from left to right in equal sections with small overlaps. Each original is also photographed in one exposure and is included in reduced form at the back of the book.

Photographs included in the original manuscript have been reproduced xerographically in this copy. Higher quality 6" x 9" black and white photographic prints are available for any photographs or illustrations appearing in this copy for an additional charge. Contact UMI directly to order.

U·M·I

University Microfilms International
A Bell & Howell Information Company
300 North Zeeb Road, Ann Arbor, MI 48106-1346 USA
313/761-4700 800/521-0600

Order Number 9127696

**A ^{195}Pt nuclear magnetic resonance spectroscopy study of the
solvolysis of sodium hexachloroplatinate by dimethyl sulfoxide**

Allbritten, Jeffery Scott, D.A.

Middle Tennessee State University, 1991

U·M·I
300 N. Zeeb Rd.
Ann Arbor, MI 48106

A ^{195}Pt NUCLEAR MAGNETIC RESONANCE SPECTROSCOPY
STUDY OF THE SOLVOLYSIS OF SODIUM HEXACHLOROPLATINATE
BY DIMETHYL SULFOXIDE

Jeffery Scott Allbritten

A dissertation presented to the
Graduate Faculty of Middle Tennessee State University
in partial fulfillment of the requirements
for the degree Doctor of Arts

May, 1991


A ^{195}Pt NUCLEAR MAGNETIC RESONANCE SPECTROSCOPY
STUDY OF THE SOLVOLYSIS OF SODIUM HEXACHLOROPLATINATE
BY DIMETHYL SULFOXIDE

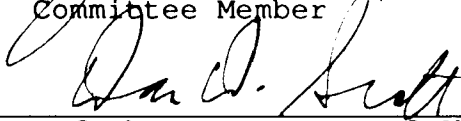
APPROVED:

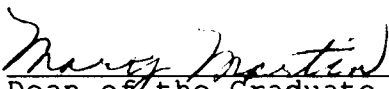
Graduate Committee:


Major Professor


Committee Member


Committee Member


Chairman of the Department of Chemistry and Physics


Dean of the Graduate School

ABSTRACT

A ^{195}Pt NUCLEAR MAGNETIC RESONANCE SPECTROSCOPY
STUDY OF THE SOLVOLYSIS OF SODIUM HEXACHLOROPLATINATE
BY DIMETHYL SULFOXIDE

Jeffery Scott Allbritten

Platinum-195 Fourier transform nuclear magnetic resonance spectroscopy was used to study the reaction of sodium hexachloroplatinate with dimethyl sulfoxide- d_6 in the mixed solvent dimethyl sulfoxide- d_6 : water, 1:2, V/V.

The reaction was observed at several temperatures over uniform time intervals to ascertain the temperature dependence of the rate of the reaction. The spectra generated were integrated to determine the extent to which the reaction had proceeded at the different temperatures as a function of time. Rate constants for the reaction at each of the temperatures were then calculated from linear regression analyses of the spectral integration values. The value at 59.4°C is $1.31 \times 10^{-4} \text{ s}^{-1}$. An Arrhenius plot of these rate constants was made and from this several kinetic activation parameters were calculated.

Finally, the reaction was submitted to long duration temperature equilibration experiments to ascertain the

Jeffery Scott Allbritten

thermodynamic equilibrium constant and therefore the molar free energy change for the reaction and any variation in this value as a function of temperature. From the temperature dependence, the molar enthalpy change for the reaction was obtained. Finally, the molar entropy change was calculated. The values at 59.4°C were 0.9 KJ mol⁻¹, -45.1 KJ mol⁻¹ and -138 J K⁻¹ mol⁻¹, respectively.

ACKNOWLEDGMENTS

I would like to sincerely thank Dr. James Howard for his patience and support throughout every stage of this work. I would also like to take this opportunity to thank Dr. Dan Scott, Dr. Roy Clark and the other members of the faculty and staff for their encouragement and input on this project. I would also wish to express my appreciation to Dr. Jack Arters for the many hours of insightful wisdom and wit which he has shared with me, and for his continuing confidence and faith in me as a scholar.

I would like to express my gratitude to the Graduate School of Middle Tennessee State University for the Doctor of Arts Fellowships which I received, and to Dr. Mary Martin and her staff for their kind words of encouragement whenever I dropped by to pay a visit.

I would also like to thank Dr. Harold Spraker, my chairman and friend, for the constant concern, encouragement and assistance which he has generously given to me from the very first day that I set foot on this campus.

While I appreciate every individual whom I have mentioned, the one person which I would like to express my deepest appreciation to is my wife, Sandie Allbritten. Her constant love and support has made it possible for me to complete this work.

TABLE OF CONTENTS

	Page
LIST OF TABLES.....	iv
LIST OF FIGURES.....	v
LIST OF APPENDICES.....	vi
Chapter	
1. INTRODUCTION.....	1
2. MATERIALS AND METHODS.....	13
3. RESULTS.....	34
4. DISCUSSION AND CONCLUSIONS.....	65
APPENDICES.....	74
LITERATURE CITED.....	102

LIST OF TABLES

Table	Page
1. Natural logarithm of reactant concentration at the different temperatures over 15 time intervals.....	50
2. Natural logarithm of reactant concentration at the different temperatures over 15 time intervals (Duplicate Experiments).....	51
3. Rate constants and statistical data from plots of $\ln[\text{reactant}]$ versus time in variable temperature experiments.....	56

LIST OF FIGURES

Figure	Page
1. Energy difference between two spin states in an applied magnetic field.....	8
2. First hour of reaction of 1/3 DMSO-d ₆ with 2/3 H ₂ O to determine suitability for kinetic study. T = 330 K.....	19
3. Third hour of reaction of 1/3 DMSO-d ₆ with 2/3 H ₂ O to determine suitability for kinetic study. T = 330 K.....	21
4. Fifth hour of reaction of 1/3 DMSO-d ₆ with 2/3 H ₂ O to determine suitability for kinetic study. T = 330 K.....	23
5. NMR spectrum of solvolysis reaction at 330 K, 8.5 min elapsed time.....	36
6. NMR spectrum of solvolysis reaction at 330 K, 59.5 min elapsed time.....	38
7. NMR spectrum of solvolysis reaction at 330 K, 93.5 min elapsed time.....	40
8. NMR spectrum of solvolysis reaction at 330 K, 127.5 min elapsed time.....	42
9. NMR spectrum of solvolysis reaction at 330 K, 161.5 min elapsed time.....	44
10. NMR spectrum of solvolysis reaction at 330 K, 195.5 min elapsed time.....	46
11. NMR spectrum of solvolysis reaction at 330 K, 229.5 min elapsed time.....	48
12. Plot of ln[reactant] versus time for solvolysis reaction at 330 K.....	54
13. Plot of natural logarithm of rate constants versus 1/temperature. (Arrhenius Plot).....	58

LIST OF APPENDICES

Appendix	Page
I. NMR spectra of solvolysis reaction at 325 K, 335 K and 340 K.....	74
Spectrum at 325 K, 8.5 min.....	75
Spectrum at 325 K, 42.5 min.....	76
Spectrum at 325 K, 93.5 min.....	77
Spectrum at 325 K, 178.5 min.....	78
Spectrum at 325 K, 246.5 min.....	79
Spectrum at 335 K, 8.5 min.....	80
Spectrum at 335 K, 42.5 min.....	81
Spectrum at 335 K, 76.5 min.....	82
Spectrum at 335 K, 110.5 min.....	83
Spectrum at 335 K, 161.5 min.....	84
Spectrum at 340 K, 8.5 min.....	85
Spectrum at 340 K, 25.5 min.....	86
Spectrum at 340 K, 42.5 min.....	87
Spectrum at 340 K, 59.5 min.....	88
Spectrum at 340 K, 76.5 min.....	89
II. Plots of natural logarithm of hexachloro platinate(IV) concentration versus time for the solvolysis reaction at 325 K, 335 K and 340 K.	90
Plot at 325 K. (First set).....	91
Plot at 325 K. (Duplicate set).....	92
Plot at 335 K. (First set).....	93

Plot at 335 K (Duplicate set).....	94
Plot at 340 K (First set).....	95
Plot at 340 K (Duplicate set).....	96
III. Plots of natural logarithm of observed rate constants versus $1000/T$. (Arrhenius plots).....	97
First set of experiments.....	98
Duplicate set of experiments.....	99
IV. Plot of natural logarithm of equilibrium constants versus $1/T$	100
Plot.....	101

Chapter 1

INTRODUCTION

Since the discovery of platinum on the South American continent by Ulloa in 1735, many uses for this relatively inert material have been found, including jewelry, high temperature resistance wires, sealed vessels for the laboratory, and as anodes for cathodic protection systems for various metallic devices¹. Other areas of interest which have been explored for this metal are its uses as a poison and its potential medicinal benefits.

Since platinum is classified as a heavy metal, much concern has been focused on its toxic effects on the body, primarily on the function of the renal system²⁻⁴. While the toxicity of this metal has been a threat to man, it is this trait which has also provided medicine with a powerful tool in the war on cancer. Several platinum derivatives have been found to exhibit strong anti-neoplastic behavior, which has led researchers to study more about this element.

The most successful and popular of the platinum anti-neoplastic agents has been "Cisplatin" or $\text{cis-Pt}(\text{NH}_3)_2\text{Cl}_2$. Research into these anticancer drugs has included the mechanism of interaction of the platinum analog and the DNA of a cell⁵⁻¹⁷. Considerable interest has also been focused into the reasons behind resistance to some of these platinum

anticancer compounds¹⁸⁻²². Another area of research involving these platinum antitumor derivatives which has evoked a great deal of interest, is the structural changes which occur to the molecules when they are placed in different environments²³⁻²⁶.

One of the most important tools used in studying metallic nuclei, including platinum, is nuclear magnetic resonance spectroscopy. Since the inception of NMR, nearly every nucleus has been investigated. Elements like tin²⁷⁻³⁶, lead^{27,28}, cadmium^{27,37}, and mercury²⁸ have been extensively studied using nuclear magnetic resonance spectroscopy.

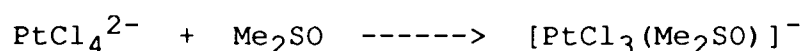
The interest in platinum-195 NMR has developed out of the search for chemotherapeutically active analogs of the drug cisplatin. Nuclear magnetic resonance spectroscopy has become the technique of choice in structural determination, and in studying reaction mechanisms for these platinum compounds due to some favorable properties of the platinum-195 nucleus³⁸. Platinum-195 has a natural abundance of 33.7%, and a relative sensitivity of 9.9×10^{-3} , while carbon-13 has a natural abundance of 1.1%, and a relative sensitivity of 1.59×10^{-2} . This combined with its nuclear spin of 1/2 has made it possible for straightforward detection under the right conditions^{38,39}. It was discerned that special precaution had to be taken when the platinum nucleus was bound to a quadrupolar nucleus, such as N-14 in

cisplatin. Kerrison and Sadler⁴⁰ reported that the quadrupole moment of N-14 leads to linewidths of ca. 200 Hz for cisplatin in DMSO. When these quadrupolar nuclei are present, the linewidths in the spectrum can become very large and make detection of the signal nearly impossible^{38,41,42}.

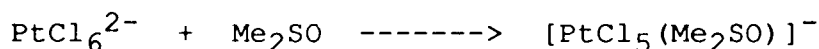
The research in this field has gone in many directions, from purely applied medicinal chemistry, to the more esoteric studies such as ligand approach and coordination to the central metal atom in the area of inorganic chemistry⁴³⁻⁴⁹. One of the major areas of research, and the one discussed in this paper, is the use of this technology to follow the solvolysis reactions of various platinum complexes. Much of the research into solvolysis has concentrated on the Pt(II) nucleus in water, and many organic solvents^{40,50-55}, while the Pt(IV) nucleus has been studied primarily in alkaline aqueous solution⁵⁶. The reason for this is that the Pt(II) nucleus is thought to be the form in which most of the chemotherapeutic activity is found, hence it has been given preferential treatment. The Pt(IV) nucleus must not be ignored as it is theorized that some of the Pt(II) compounds undergo a conversion to the Pt(IV) analog in solution²³. Thus, any subsequent reaction with the solvent may serve either to enhance the drugs beneficial properties, or to destroy these desired properties. Knowledge of the reactivity of the Pt(IV)

nucleus with various solvents would be extremely useful in designing a drug which will remain active in the different environments in which it may find itself.

Pesek and Mason³⁹ reported on a study of tetra-n-butylammonium salts of hexachloroplatinate, PtCl_6^{2-} , and tetrachloroplatinate, PtCl_4^{2-} , in various nonaqueous solvents in which they state that the PtCl_4^{2-} ion underwent solvolysis in dimethyl sulfoxide within thirty minutes of preparation. This rapid reaction with this Pt(II) compound



does not lend itself well to a slow, careful study using NMR. They go on to say however, that the PtCl_6^{2-} ion remained stable at room temperature, but underwent solvolysis when subjected to elevated temperatures for various lengths of time. It is this reaction of the PtCl_6^{2-} ion with dimethyl sulfoxide which is studied here



utilizing variable temperature platinum-195 NMR spectroscopy. By monitoring it over several temperatures, data were obtained to establish rate constants at each temperature, the activation energy and activation parameters, and the thermodynamics for this reaction.

The major hypothesis of this study was that dimethyl sulfoxide will act as an S-donor ligand and attack the

platinum nucleus in the hexachloroplatinate ion, displacing a chloride thereby changing the magnetic environment about platinum. It is this change in magnetic environment that will be seen either as a shielding or a deshielding effect, causing the appearance of another peak in the nuclear magnetic resonance spectrum of the platinum nucleus. The intensity of this new peak should increase as the reaction continues to completion. By measuring the relative intensities of these two peaks over several time intervals one should be able to calculate the rate constant for this reaction.

To fully understand the significance of this change in the magnetic environment about the platinum nucleus and the resulting resonance spectrum, one must first appreciate the nature of nuclear magnetic resonance spectroscopy. A brief discussion of the principles of nuclear magnetic resonance is given to assist the reader in appreciating the material presented in this work.

To understand nuclear magnetic resonance, one must begin with an examination of the nucleus of an atom⁵⁷. The nucleus of any atom consists of neutrons and protons which have a spin quantum number of $1/2$ respectively. The proportions of neutrons and protons in a nucleus determines the value of the nuclear spin quantum number, I . If the neutrons and protons are in equal proportions then the spins will all be paired resulting in a nuclear spin quantum

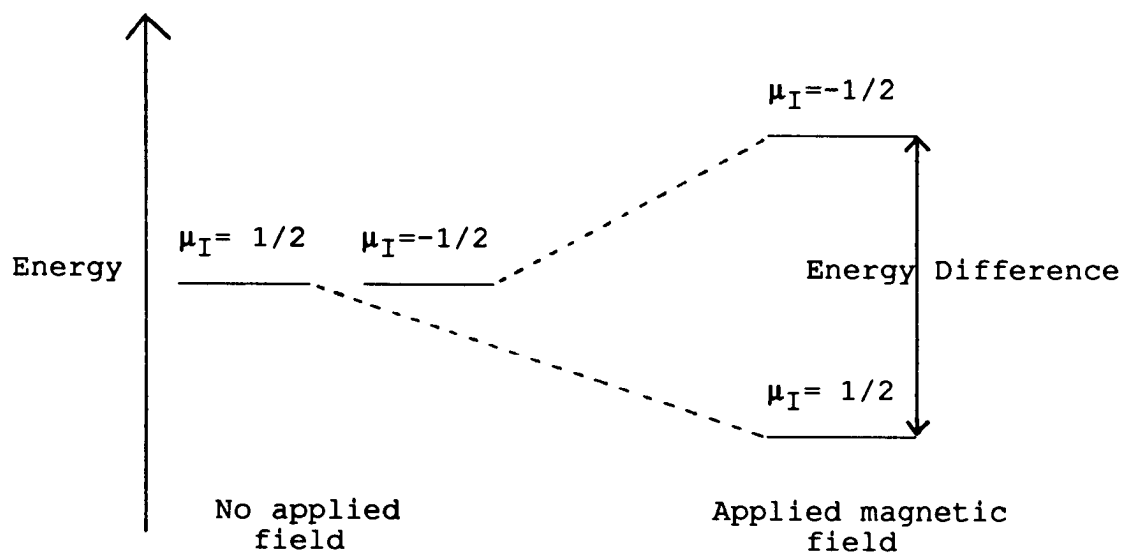
number of zero. If the proportions are not equal, then the spins will not be paired resulting in a nuclear spin quantum number $I > 0$. When this situation is present, the nucleus will possess a magnetic moment and will behave like a small bar magnet, subject to all of the magnetic and electrical lines of force present in its environment.

When a nucleus with $I > 0$ experiences no external magnetic field, the nuclear magnetic moment vector may take on an infinite number of spatial orientations. But, when this nucleus is placed in a magnetic field, it is forced to take on only certain allowed orientations dictated by μ_I , the nuclear spin angular momentum quantum number, whose allowed values are $I, I - 1, \dots, (-I + 1), -I$. Because the platinum nucleus has spin $1/2$, the remainder of this discussion will be restricted to nuclei of spin $1/2$.

These nuclei have two spin states. One, $\mu_I = +1/2$, has the nuclear magnetic moment vector aligned with the applied magnetic field and the other, $\mu_I = -1/2$, has it opposed to the applied magnetic field. The orientation of the nuclear magnetic moment vector with $\mu_I = +1/2$ is lower in energy than the orientation with $\mu_I = -1/2$. This difference in energy of spin states is the property that is used in nuclear magnetic resonance spectroscopy. (Figure 1)

A nucleus can be forced to change spin states when a quantity of energy equal to the difference in energy of the two spin states is absorbed. In an NMR experiment, radio

Figure 1. Energy difference between two spin states in an applied magnetic field.



frequency radiation is focused on the nuclei to induce the transition between the two spin states⁵⁸. When the transition from the low energy spin state to the high energy spin state occurs, the frequency of radiation which is absorbed is measured. Each nucleus has a particular frequency of radiation associated with its transition depending upon the environment of the nucleus. By measuring the frequency of radiation absorbed by the sample, a spectroscopist can obtain information about the environment of a particular type of nucleus.

A nuclear magnetic resonance spectrometer generates a constant magnetic field, B_0 , which causes the nuclei in a sample to orient themselves either with or against this applied field. According to the Boltzmann distribution, a population of nuclei with spin $1/2$ will have an excess of the nuclei in the lower energy state aligned with the applied field. This excess results in a net magnetization vector which is aligned with the field. When the B_0 field alone is applied, there is no net energy absorption. When the nuclei are forced out of this alignment by the application of a magnetic field, B_1 , perpendicular to B_0 , a component of this net magnetization vector causes an induced current in the receiver coil yielding the characteristic NMR signal.

In addition to the nuclei orienting in the field B_0 , they precess about the field at a speed termed the Larmor

frequency. The Larmor frequency of each nucleus depends upon the applied field strength and the magnetogyric ratio of the nucleus, a constant characteristic of the nucleus. In traditional nuclear magnetic resonance experiments, a circularly polarized radio frequency field, B_1 , is continuously applied perpendicular to the applied field B_0 . The frequency of the B_1 field is varied until it matches the Larmor frequency of the precessing nuclei. When this frequency of radiation is attained, the magnetic component of B_1 interacts with the nuclei's net magnetization vector delivering a torque on this vector causing the spin to flip to the higher energy state in opposition to the applied field B_0 . It is this absorption of energy from the plane in which the receiver coil lies which is measured and plotted as a signal in a frequency spectrum.

As was stated previously, traditional NMR experiments utilized a circularly polarized radio frequency field which was gradually increased through the entire frequency region until resonance with the Larmor frequency of the nucleus occurred. This approach is very time consuming, especially if many nuclei are present all with different resonance frequencies. A significant improvement to this method of frequency scanning was implemented in the mid-1960's with the advent of pulse radio frequency technology. Quite simply, instead of slowly scanning the frequency spectrum searching for the resonance frequency, one can deliver a

single, high power burst of radiation for a very short time and excite all of the nuclei simultaneously. Shortly after the pulse is turned off, the receiver is turned on to measure the composite of the signals from the various nuclei present. Obviously, this presents some difficulty in interpretation when many nuclei are present, so a Fourier transformation is utilized to convert the resulting time domain into the usual NMR spectrum (frequency domain). This new technology has opened the door to many new applications of nuclear magnetic resonance spectroscopy.

The subject of conducting nuclear magnetic resonance research on metallic nuclei, such as platinum, is just one of the areas of interest which has been aided by the new technology. With the advent of FT NMR, the scientific world began to devote a great deal of time and resources to this emerging frontier³⁸.

The solvolysis reaction studied here is of particular significance since many of the platinum anticancer compounds are being administered in aqueous dimethyl sulfoxide. This information may prove useful to those in the scientific community who are studying the mechanism of action of anti-cancer drugs.

This study is also intended to demonstrate to the student of chemistry, the utility of non-proton nuclear magnetic resonance spectroscopy in the chemical laboratory. Therefore, the focus of this study is to provide accurate

and relevant information, as an instructional aid, by application to the study of a very significant process in chemistry today.

Chapter 2

MATERIALS AND METHODS

Materials

Sodium hexachloroplatinate hexahydrate, lot number 02615KW, was purchased from Aldrich Chemical Company in Milwaukee, WI, and used without further purification. Dimethyl sulfoxide- d_6 , lot number NS0789, was purchased from ISOTEC Inc., in Miamisburg, OH. The water used in this study was deionized by a Corning water purifier, model number LD-5a.

A 1.0 M sample of $\text{Na}_2\text{PtCl}_6 \cdot 6\text{H}_2\text{O}$ in D_2O , was prepared by weighing out 281 mg of the dry, crystalline material directly into an NMR tube. Then, 0.5 mL of deuterium oxide was added to the tube yielding a 1.0 M standard sample.

Methods

Spectra were obtained using a Bruker AC 200 Fourier transform nuclear magnetic resonance spectrometer, operating at an applied field, B_0 , of 4.7 T. The spectrometer is equipped with a 5 mm broadband probe (14 MHz to 90 MHz), a Bruker model EC01 variable temperature unit, and an Aspect 3000 computer with coprocessor for data analysis and manipulation.

The spectrometer was tuned to 43.0 MHz for the platinum-195 resonance. This was accomplished by reading a C-13 tuning file, changing SFO to 43.0 MHz, and by procedures outlined in one of the manuals for the instrument.

Once the proper resonance frequency was established, the numerous acquisition parameters, such as frequency offset, sweepwidth, relaxation delay, and pulsewidth were determined using the 1.0 M sample of sodium hexachloroplatinate in deuterium oxide. This sample was placed into the magnet with the following initial acquisition parameters entered: relaxation delay(RD) = 2.0 s; frequency offset(O1) = -30,000 Hz; sweepwidth(SW) = 125,000 Hz; number of scans(NS) = 500; data array size(SI) = 8K; pulsewidth(PW) = 2.1 μ s. Other parameters were left at their default values.

Upon pulsing the one molar standard in D₂O 500 times with these parameters, it was apparent, from the strong peak observed, that the instrument was properly adjusted to perform platinum-195 spectroscopy on this compound. Once this was determined, it was then necessary to fine tune these parameters by subjecting this compound, in the appropriate reaction solvents, to the same experiment as the original standard. It was also necessary to determine if the solvolysis reaction occurred at a rate suitable for a kinetic study by NMR spectroscopy. This suitability criterion would be determined by subjecting a reaction

mixture to a long-term NMR experiment and watching the change in the resulting spectra as a function of time. If the reaction occurred too rapidly it would be extremely difficult to observe changes in ratios of peak heights corresponding to the reactants and the products. If this turned out to be the case then this reaction would be inappropriate for an NMR kinetic study.

A 0.9 M sample of $\text{Na}_2\text{PtCl}_6 \cdot 6\text{H}_2\text{O}$ in $2/3 \text{ H}_2\text{O}$ and $1/3 \text{ DMSO-d}_6$ by volume was prepared by weighing out 183 mg of the crystalline hexachloroplatinate material directly into an NMR sample tube. A 215 μL aliquot of H_2O was added to the dry hexachloroplatinate in the tube and agitated until the sample dissolved. A 110 μL aliquot of DMSO-d_6 was added to the tube, for a final volume of 360 μL , just before the sample mixture was ready to be placed into the NMR for observation. Care had to be taken as to the time of the addition of the DMSO-d_6 , as the literature indicated that this reaction did occur at room temperature within approximately 30 min of combination of reactants³⁹.

Once the DMSO had been added, the sample was well mixed by shaking and placed into the magnet for observation. The following modifications to the list of acquisition parameters were made before the experiment began: $\text{RD} = 7.0 \text{ s}$; $\text{Temperature(TE)} = 330 \text{ K}$. The reason for the increase in the relaxation delay was to insure complete "ringdown". The temperature of 330 K was chosen at random with the

constraint of choosing a temperature above 298 K to insure the ability of testing this reaction at various temperatures, but also below the boiling point of the solvent.

An automation program was written which reset the instrument after a single 500-pulse experiment. The program was designed to save the free induction decay of an experiment to the hard disk drive as soon as it was complete and to then wait a specified time interval before beginning another data collection sequence. This was necessary as the reaction needed to be followed over a long time interval to determine the suitability of the utilization of nuclear magnetic resonance spectroscopy for a kinetic study of this reaction. A delay of one hour was entered and the number of data collection cycles was set to five. With a relaxation delay of 7.0 s, one data collection cycle would take approximately one hour. Therefore with five data collection cycles and the five delay cycles this experiment would span 10 hrs.

The instrument was activated and the experiment was allowed to run to completion. The five resulting spectra revealed the gradual decrease in intensity of a downfield peak, corresponding to unreacted Na_2PtCl_6 , with a concomitant increase in intensity of a peak approximately 1000 ppm upfield, corresponding to a solvolysis product, with time. Upon investigation of the five resulting

spectra, it was determined that this reaction occurred at a rate which made it suitable for performing a kinetic study using platinum-195 NMR spectroscopy (see figures 2-4 for the first, third and fifth spectra of the series).

Further adjustments to the list of acquisition parameters were now made from the information received from these five spectra. The sweepwidth (SW) was reduced to 62,500 Hz and the frequency offset (O1) was moved to 7,700 Hz to center each spectrum between the reactant and product peaks. The instrument was zeroed to the frequency at which the peak of the original standard, 1.0 M sodium hexachloroplatinate in deuterium oxide, first appeared.

All of the parameters were now established except for the optimal pulsewidth for the platinum-195 nucleus. The desired pulse is a compromise between receiving the best signal to noise ratio in the spectrum and the time required to collect the data. A 30° pulse is normally best suited to give adequate signal to noise and allow more rapid data acquisition.

To determine the pulsewidth which delivers a 30° pulse, it was first necessary to determine the pulsewidth that would deliver a 90° pulse. The 90° pulse for the platinum-195 nucleus was determined by using a program called PW90 in the catalog of programs provided with the instrument. A series of successive increases and decreases of the pulsewidth led to the value of $PW = 23.5 \mu s$ for a 180°

Figure 2. First hour of reaction in 1/3 DMSO-d₆ plus 2/3 H₂O
to determine suitability for kinetic study.
T = 330 K

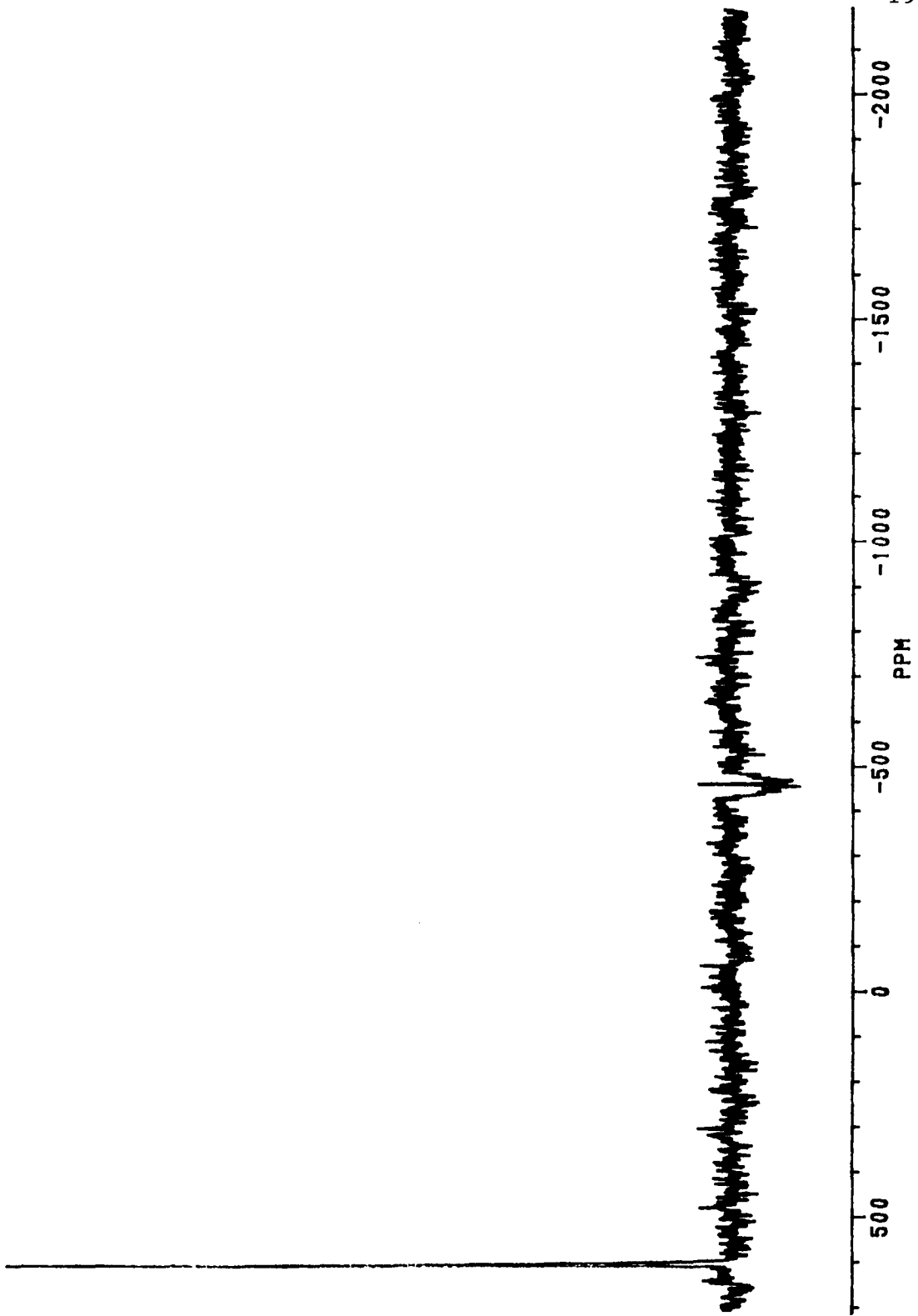
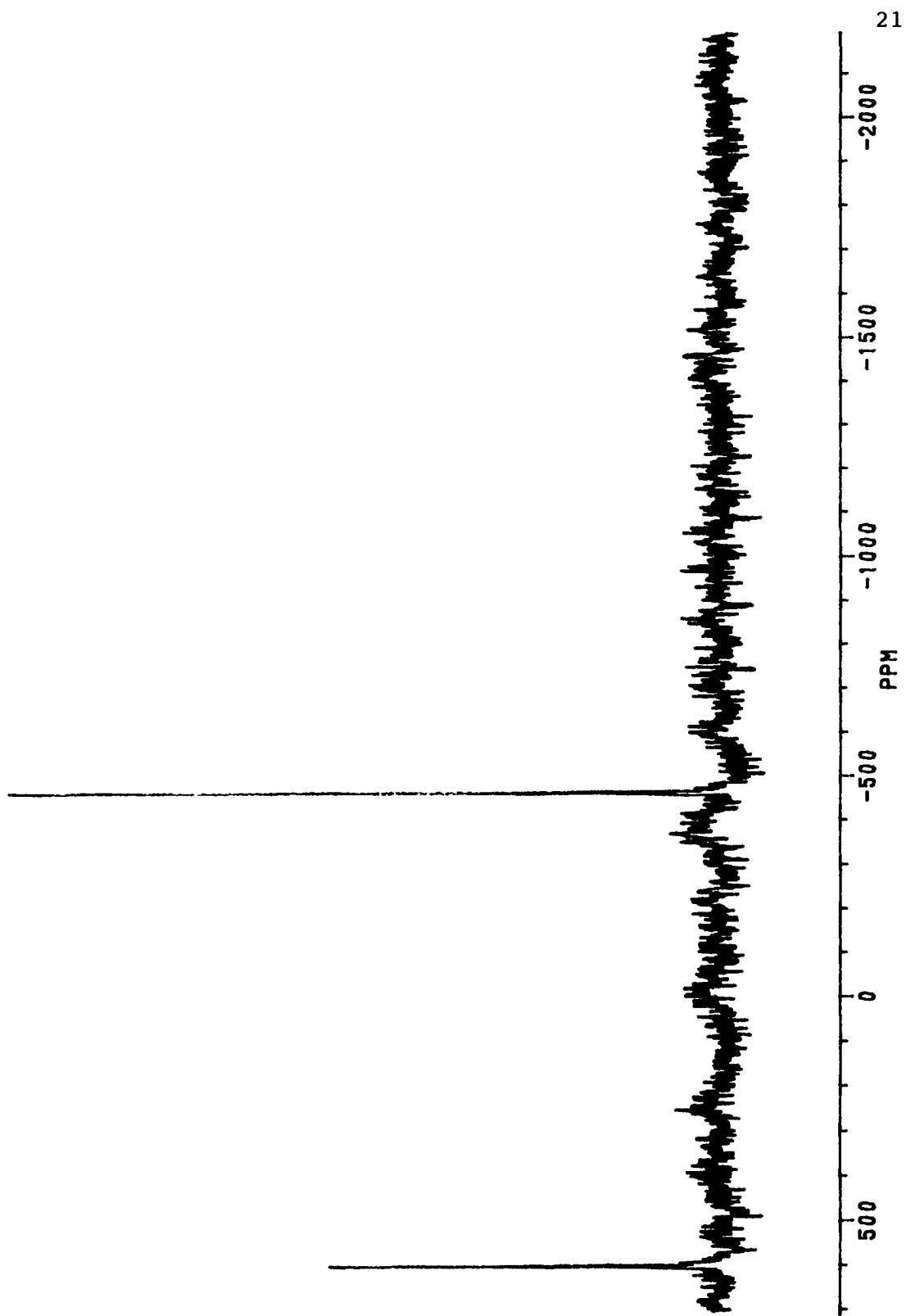
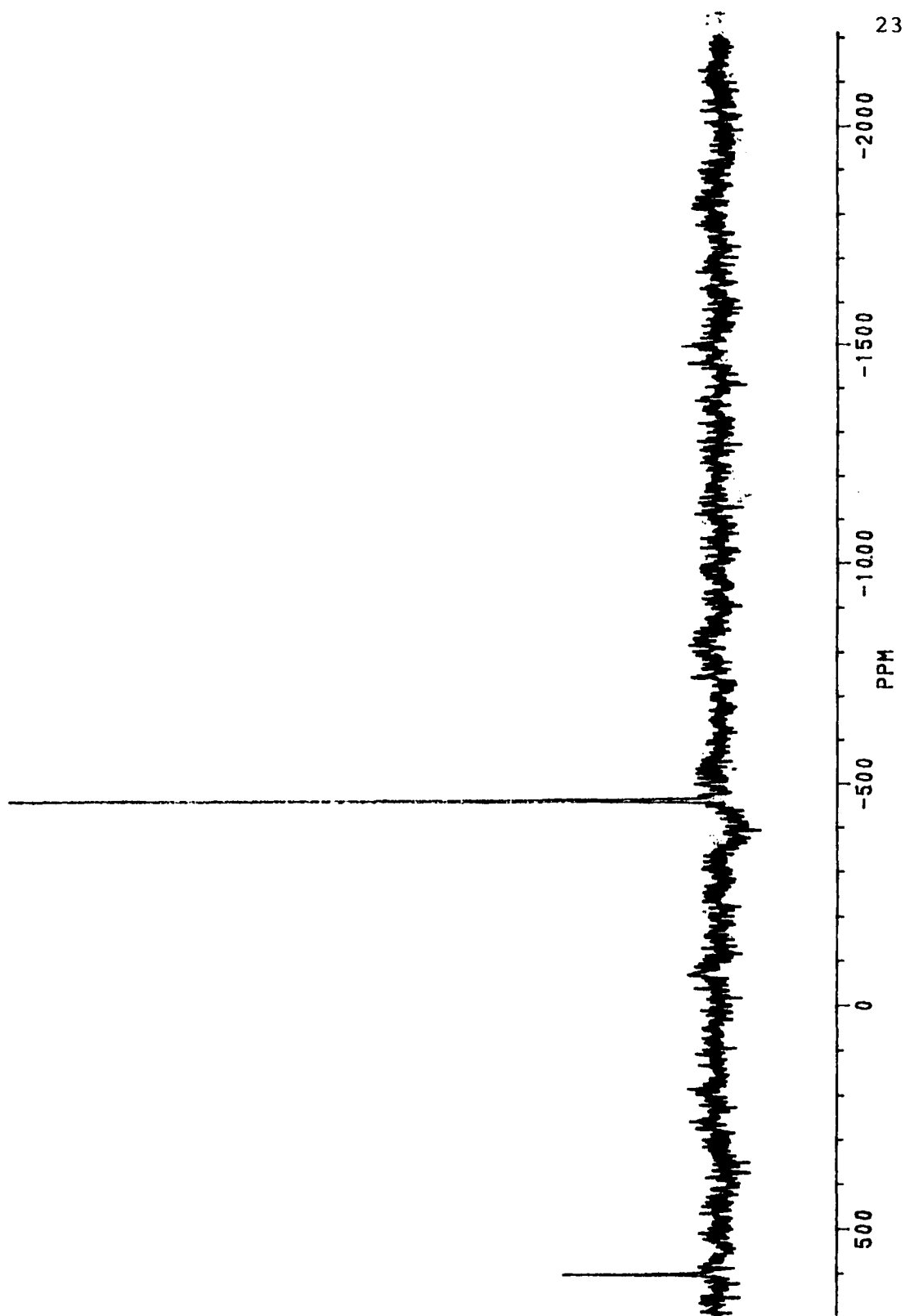


Figure 3. Third hour of reaction in 1/3 DMSO-d₆ plus 2/3 H₂O
to determine suitability for kinetic study.
T = 330 K.



21

Figure 4. Fifth hour of reaction in $1/3$ DMSO- d_6 plus $2/3$ H_2O
to determine suitability for kinetic study.
 $T = 330$ K.



pulse. From this value the PW for a 90° pulse is calculated to be $11.25 \mu\text{s}$. Since a 30° pulse was desired, a PW of $4.0 \mu\text{s}$ was set into the list of acquisition parameters along with a relaxation delay of 2.0 s . The list of acquisition parameters was now complete and the kinetic study could proceed.

Based on the data obtained, it was decided that this reaction could be followed for approximately five hours. This corresponded to the time the reaction apparently had reached completion. It was also decided that four temperatures, 325 K , 330 K , 335 K , and 340 K would be used to study this reaction. The decision to use this moderate temperature range was made based upon previous experience with this material and the knowledge that activation energies and other activation parameters can be temperature dependent. Carrying out this reaction at four different temperatures would allow an Arrhenius plot to be made and the activation energy to be determined from the slope.

A fresh sample of the reaction mixture was used for each temperature at which the reaction was studied. The experiment required at least 1.5 g of the sodium hexachloroplatinate hexahydrate.

The first temperature at which the study began was the temperature at which the suitability experiment was run, 330 K . A 0.9 M sample of sodium hexachloroplatinate was prepared by weighing out 183 mg of the crystalline material

directly into the NMR sample tube. Next, a 215 μL aliquot of H_2O was added and the tube was agitated until the material was dissolved. The temperature controller was set to 330 K and allowed to equilibrate at this temperature for approximately 30 min. The automation program which was described previously was modified for a delay of 5.0 s between data collection cycles, and the number of experiments was increased from five to 15. With a relaxation delay of 2.0 s, and 500 scans per experiment, each experiment took approximately 17 min to complete. This was determined in a separate experiment to give adequate signal to noise. Therefore, 15 experiments would allow this reaction to be studied for approximately 4.5 hr at each temperature.

When all of the acquisition parameters on the instrument had been entered and everything was ready to go, a 110 μL aliquot of DMSO-d_6 was added to the tube. The tube was shaken to insure proper mixing of all components. Then, it was immediately placed into the magnet, a lock signal obtained, the magnet shimmed, and the experiment begun. This precaution was taken to insure a consistent initial reaction time for all of the experiments.

After the 15 separate 500-pulse experiments on this first sample at 330 K were complete, the tube was removed from the magnet and the next sample to be run was prepared. The variable temperature controller was set to 335 K and the

automation program was set for another 15-experiment data acquisition cycle. This procedure was conducted twice at each of the four temperatures to insure reproducibility of the results.

Once an experiment at a certain temperature was complete, the free induction decay from each of the 15 data acquisition cycles in the experiment was subjected to an exponential multiplication routine with a line broadening parameter of 50 Hz. This was done to reduce the noise which was received during the acquisition cycle. This exponentially multiplied data was then subjected to a Fourier transformation routine which yielded the characteristic nuclear magnetic resonance spectrum. The spectrum which was received at this point required the application of a phase correction routine to bring the peaks into consistent phase one with another. A zero-order phase correction was made on the larger peak in the spectrum followed by a first-order phase correction on the smaller peak in the spectrum. These two parameters were manipulated interactively until a compromise between the two was reached.

The next problem with the spectra of this reaction was the persistent presence of "wavy" baselines. To counter this, a baseline correction routine in the software was utilized. There were two baseline correction routines available, one which fitted the baseline to a cubic spline

algorithm, and the other which fitted the baseline to different polynomial algorithms. The cubic spline algorithm turned out to be the best for flattening the baseline for these spectra.

The baseline correction routine is available either 1) as a completely automated routine which picked random points from the baseline followed by mathematical analysis, or 2) in an interactive mode in which the points were picked manually and then subjected to analysis. Most of the baseline correction done in this research was the manual manipulation mode. To use the cubic spline algorithm with manual point picking successfully, it was necessary to pick points from the phased spectrum properly. Great care was taken to insure that the points were in the baseline noise and not at the upper or lower limits of this noise. Once the points were chosen, they were analyzed using a cubic spline algorithm and a new baseline was generated. Very often this procedure was not completely successful with one trial, so that several baseline corrections were usually combined to yield the flattest baseline. When the final spectra were ready, they were plotted on a Graphtec MP3200 plotter which was interfaced with the Aspect 3000 computer.

Once all of the reactions were carried out, and the spectra had been phased and baseline corrected, the analysis of the kinetics of this solvolysis reaction began. Since one of the reactants in this reaction was the solvent, it

was assumed that this reaction was pseudo first-order in the platinum compound. With this assumption made, it was now possible to determine the rate of this reaction by following either the appearance of product or the disappearance of the reactant and focusing on the following kinetic relationship⁵⁹:

$$-\frac{d[\text{reactant}]}{dt} = k_{\text{obs}}[\text{reactant}].$$

When both sides of this differential equation are integrated, the following relationship is obtained:

$$\ln[\text{reactant}] - \ln[\text{reactant}]_0 = -k_{\text{obs}}(t - t_0)$$

where $[\text{reactant}]_0 = 1$ at $t_0 = 0$. Therefore a plot of $\ln[\text{reactant}]$ versus time should yield a straight line. The slope of the graph equals the negative of the observed rate constant.

It was now necessary to determine the decrease in the reactant concentration over time in each experiment to be able to provide data for the plot.

To determine the change in reactant concentration as a function of time in the reaction, it was necessary to measure the change in intensity of the resulting reactant and product peaks in each spectrum throughout the course of the reaction. This was accomplished by performing an integration of each spectrum to determine the area under the

peaks which were generated.

The integration of the reactant and product peaks was done by using the integral function subroutine of DISNMR89 running on the ASPECT 3000 computer, applied on phased and baseline corrected spectra. An interval width of 100 Hz about each peak was chosen to insure uniform treatment of all peaks in the various spectra. The integration was initiated by placing the computer cursor 50 Hz downfield from a peak and zeroing the integral at that point. The integral function was then maneuvered through the peak and re-zeroed at a point 50 Hz upfield from that peak. This procedure was carried out for both the reactant and product peaks. The bias and the slope of the entire integral were then adjusted to the best of the operator's ability when necessary. Quite often the final result was a compromise between an over estimation of the area of one peak and an under estimation of the area of the other peak. This was a source for random error in the data. It was dealt with by reaching a high degree of precision and consistency in the operator's technique. Regardless, some of the data points which were generated during the data analysis phase of this research had to be treated as outliers during the linear regression analysis. The mathematical basis for this treatment is discussed later.

As the integration of the peaks for a particular temperature experiment was carried out, the area of the

reactant peak was arbitrarily set to one, so that the computer would calculate the area of the product peak relative to the reactant peak. This allowed for the generation of a ratio of the product to reactant peaks from which the concentration of the reactant species could be calculated. The concentration of the reactant species in the reaction mixture was calculated using the following mathematical relationship:

$$[\text{reactant}] + [\text{product}] = [\text{reactant}]_0 = 1$$

at time $t = 0$.

But,

$$[\text{product}]/[\text{reactant}] = \text{ratio},$$

So upon substitution,

$$[\text{reactant}] + (\text{ratio})[\text{reactant}] = 1.$$

Therefore,

$$[\text{reactant}] = 1/(1 + \text{ratio}).$$

From the ratio of the product to the reactant peak, it was now possible to measure the decrease in the concentration of the reactant species over the course of the reaction.

The ratios obtained from the 15 experiments performed twice at each temperature were then entered into a Microsoft WorksTM spreadsheet template which had been programmed to

perform linear regression analysis on the data. Since the data were to be plotted as $\ln[\text{reactant}]$ versus time, the raw x-axis data were entered as the midpoint of the appropriate 17-min interval at which the data had been gathered. The raw y-axis data were entered as the ratio of $[\text{product}]/[\text{reactant}]$ and converted to $\ln[\text{reactant}]$ by simple reprogramming of the spreadsheet.

A linear least squares regression was performed on the resulting data to determine the degree of agreement of the experimental data with the kinetic assumption made at the outset of the project, i.e., first-order in reactant. As was stated earlier, due to noise in the baseline resulting in error in the integration of the peaks, some data points had to be removed from the plots because they were spurious in nature and could be considered as statistical outliers⁶⁰. As Benson indicates, if the removal of the outliers yields a better model, then one is justified in removing those data points from the set of statistics. The appearance of such points was totally random, and their removal yielded improved correlation coefficients resulting in more accurate rate constant calculations. The results from the kinetic experiments and the thermodynamic experiments will be presented in the next chapter.

When the rate constants for each temperature had been calculated, they were then entered into a spreadsheet which plotted the $\ln(k_{\text{obs}})$ versus $1/\text{temperature}$. A linear

regression was performed on this data and the slope was used to calculate the activation energy of the reaction along with various other activation parameters.

The last question which needed to be addressed was that of the reversibility of this reaction. Was the reaction completely reversible or was there such a high activation barrier that the reverse reaction was highly unfavored? To study this question, several of the reaction mixtures which had been stored at room temperature for approximately eight weeks in their NMR tube, were placed into the magnet at 330 K and a spectrum obtained. The presence of an equilibrium condition would allow for the calculation of a thermodynamic equilibrium constant from a ratio of the product to the reactant peaks. This equilibrium constant, K_{eq} , would allow the free energy, ΔG° , to be calculated from the following thermodynamic relationship:

$$\Delta G^{\circ} = - RT \ln K_{eq}.$$

To accurately determine all of the thermodynamic parameters for this reversible reaction, it was necessary to subject a reacted sample to a long-term, gradual, variable temperature series to detect any temperature dependence of the equilibrium constant. This experiment was performed on one of the previously reacted samples by utilization of the same variable temperature computer program used to conduct the kinetic portion of this project.

This experiment was initiated by setting the variable temperature controller to 325 K and allowing it to equilibrate for approximately 30 min before the sample was placed into the magnet. The programs' acquisition parameters were set to allow a seven-hour equilibration period at each temperature in the increasing series 325 K, 330 K, 335 K, and 340 K, while gathering data every hour. This allowed sufficient time for the sample to equilibrate at each of the temperatures, to verify that equilibrium had been reached, and for any temperature dependence of the equilibrium constant to be determined.

Chapter 3

RESULTS

As was stated in the previous chapter, the first temperature chosen to begin the kinetic experiments was 330 K. The parameters were entered into the instrument and an automation program was activated to begin the data acquisition. Each of the 15 data collection cycles was 17 min in length. The time of the experiment for kinetic analysis was taken as the midpoint of the 17-min time interval.

The following seven figures are from this first kinetic experiment (Figures 5-11). In figure 5, it was apparent that very little reaction had taken place since there was only a small product peak at -450 ppm. At this temperature, there was a significant induction period before the reaction began. This induction period was more pronounced at 325 K and decreased at the two higher temperatures used for the kinetic experiment. This series of spectra is typical of the behavior of this reaction, showing the decrease in reactant concentration and concomitant increase in product concentration.

The data for this temperature are illustrated as an example of the behavior of this reaction at the various temperatures. The spectra obtained at the other

Figure 5. NMR spectrum of solvolysis reaction at 330 K,
8.5 min elapsed time.

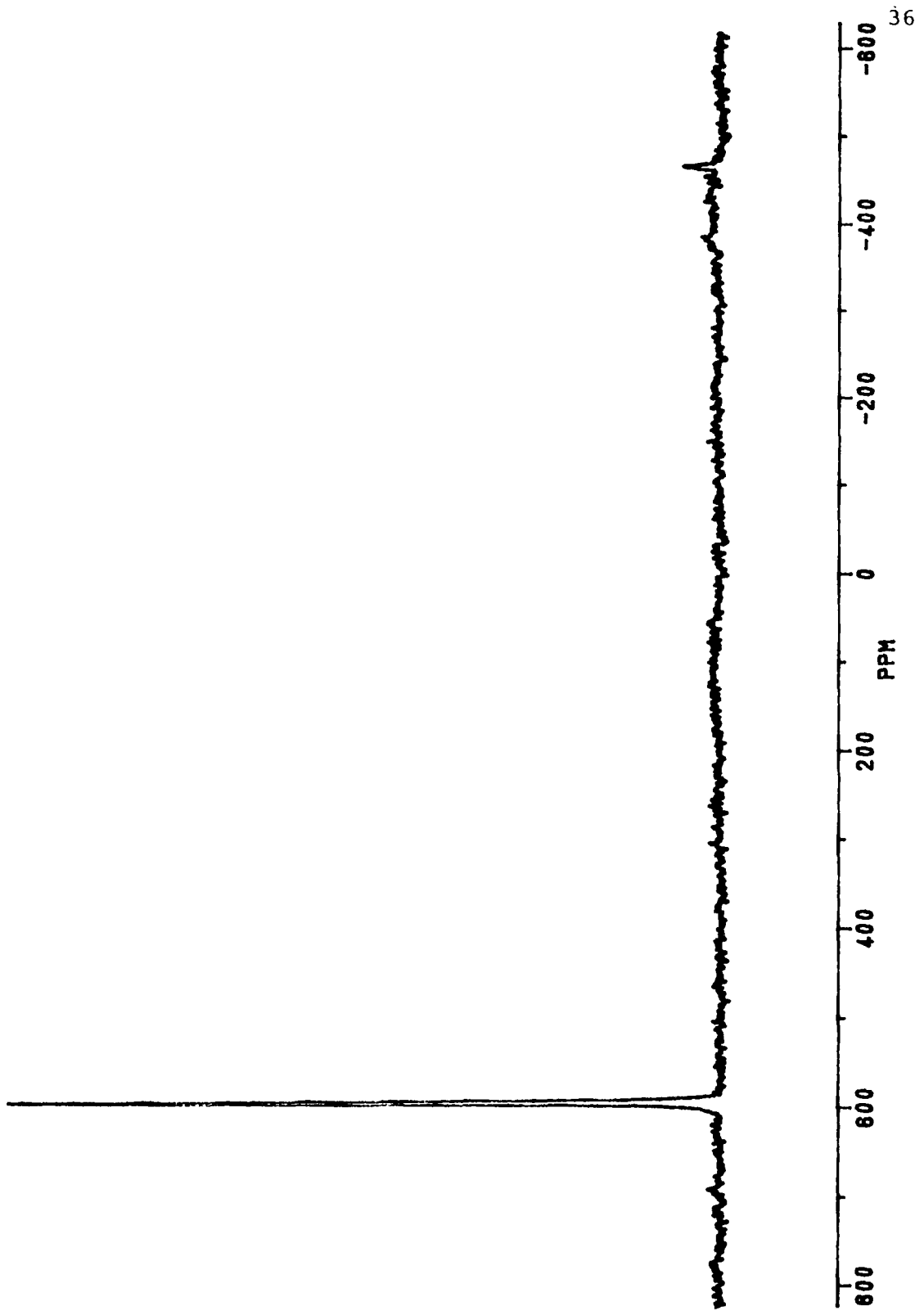


Figure 6. NMR spectrum of solvolysis reaction at 330 K,
59.5 min elapsed time.

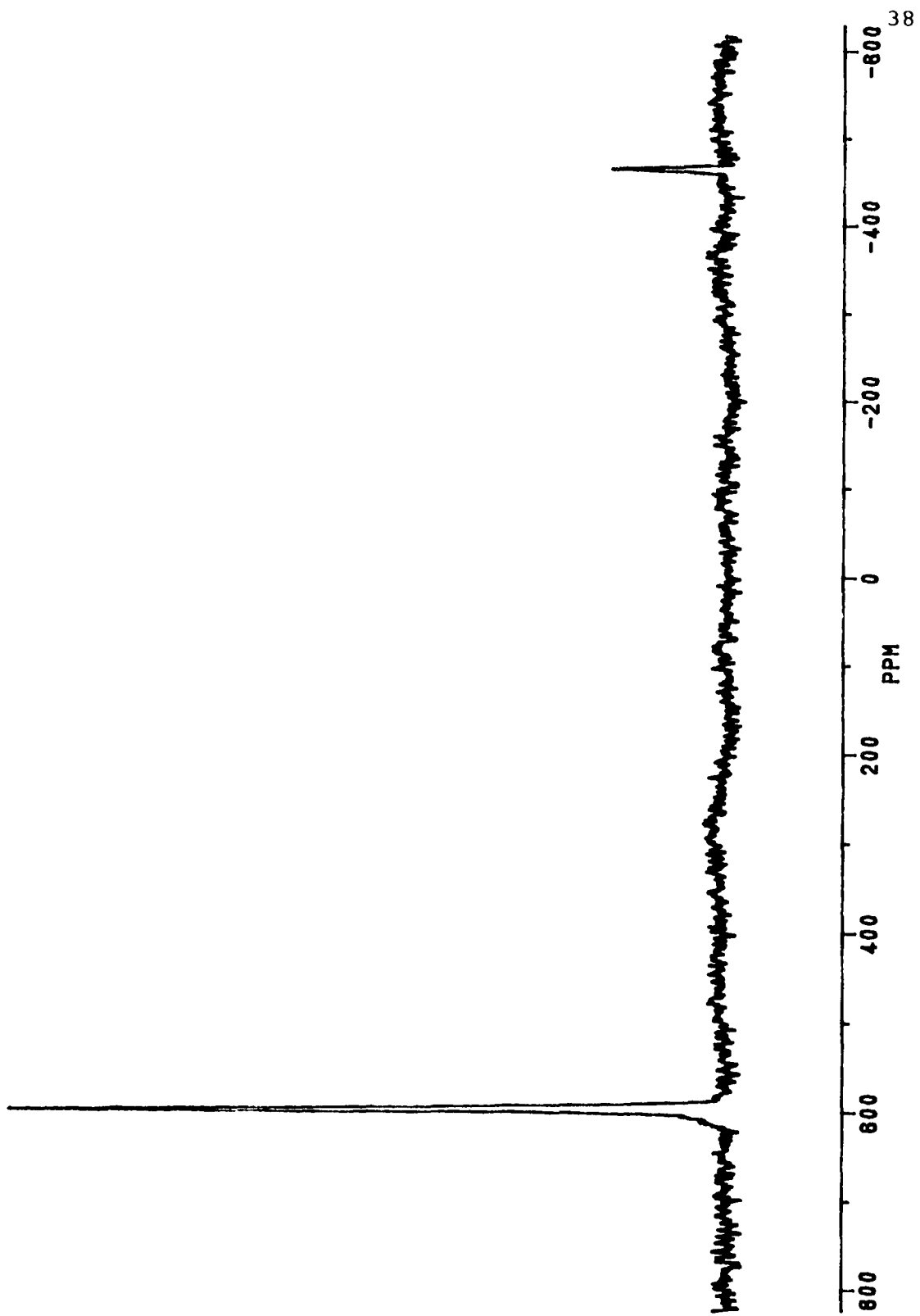


Figure 7. NMR spectrum of solvolysis reaction at 330 K,
93.5 min elapsed time.

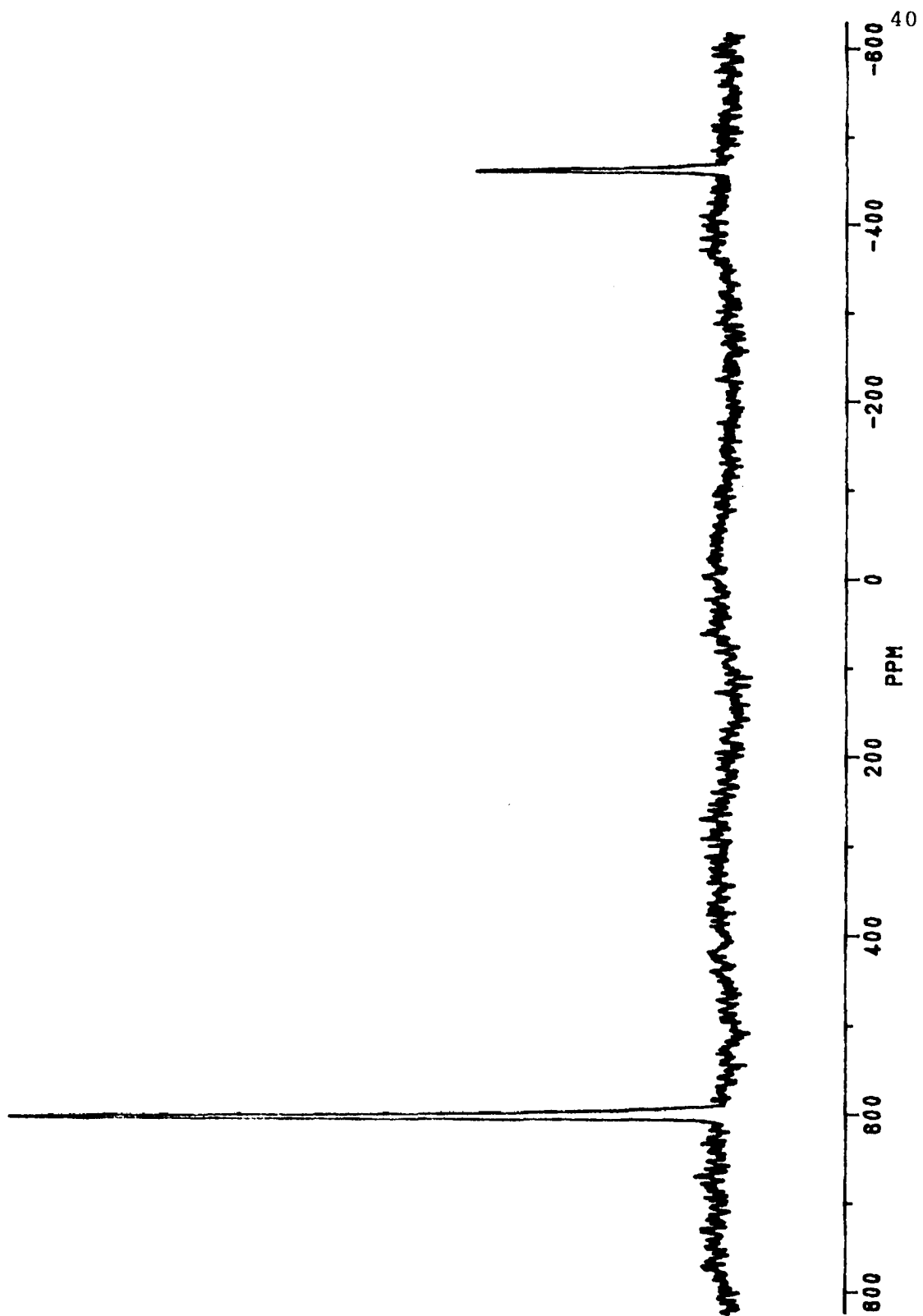


Figure 8. NMR spectrum of solvolysis reaction at 330 K,
127.5 min elapsed time.

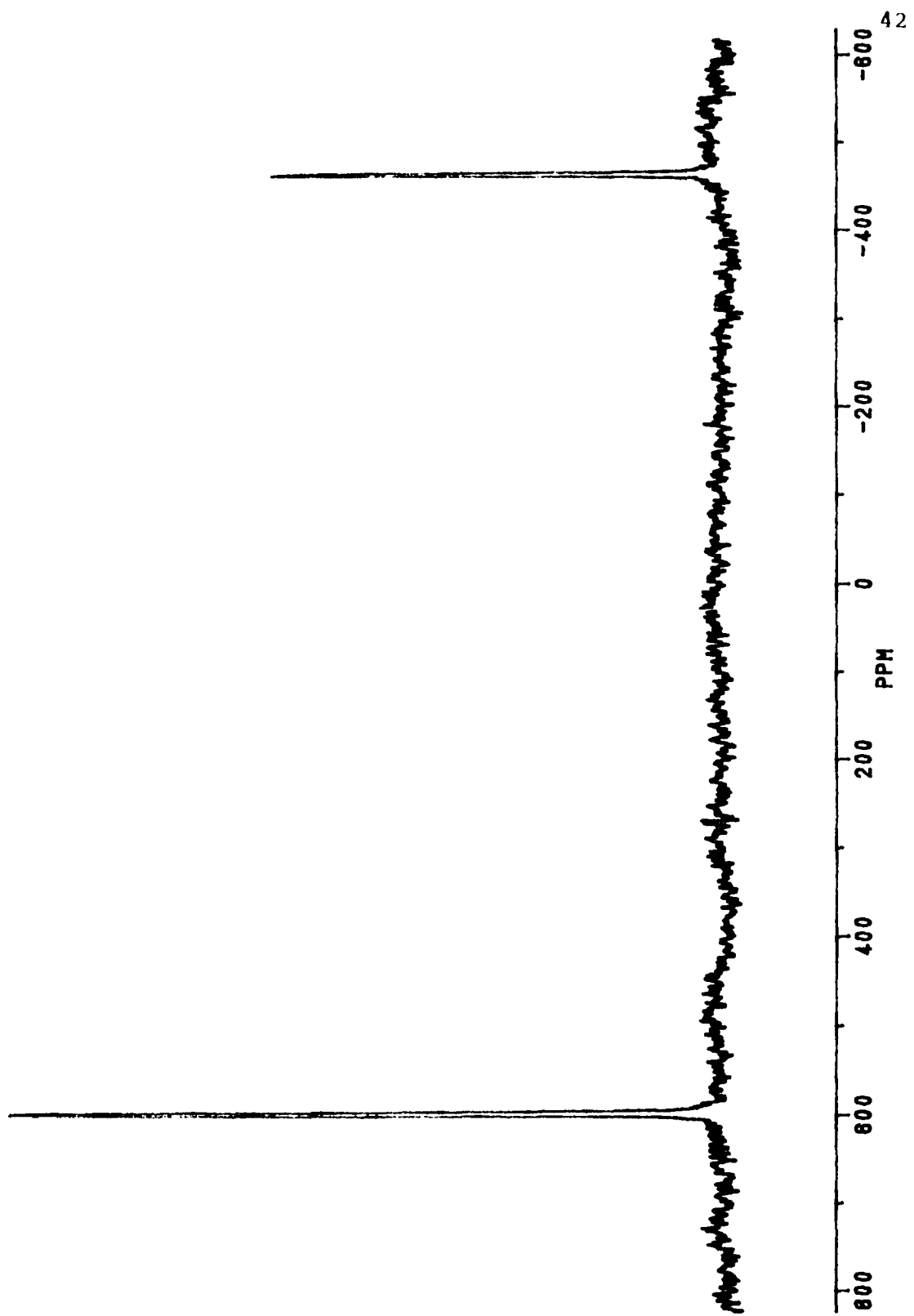


Figure 9. NMR spectrum of solvolysis reaction at 330 K,
161.5 min elapsed time.

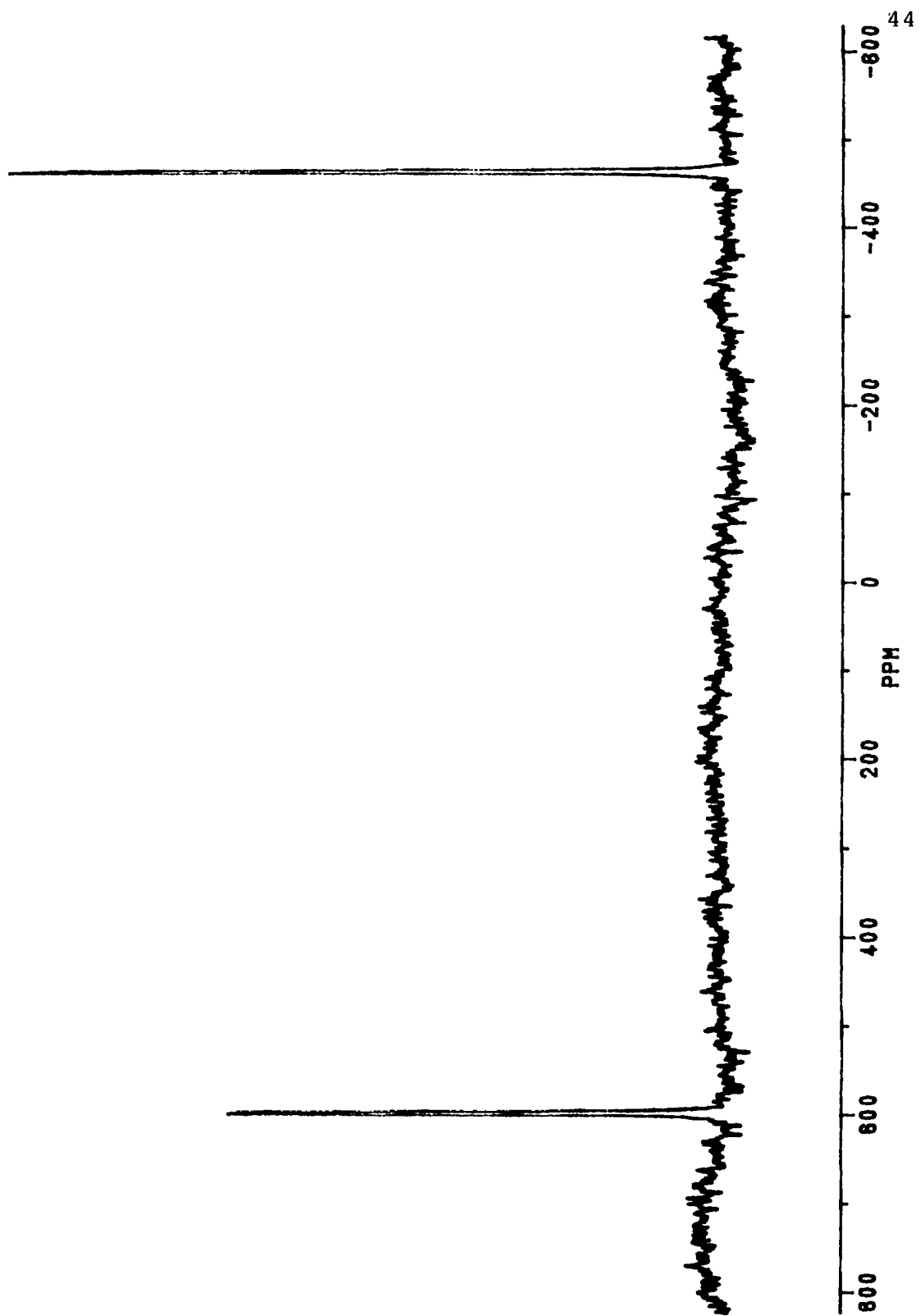


Figure 10. NMR spectrum of solvolysis reaction at 330 K,
195.5 min elapsed time.

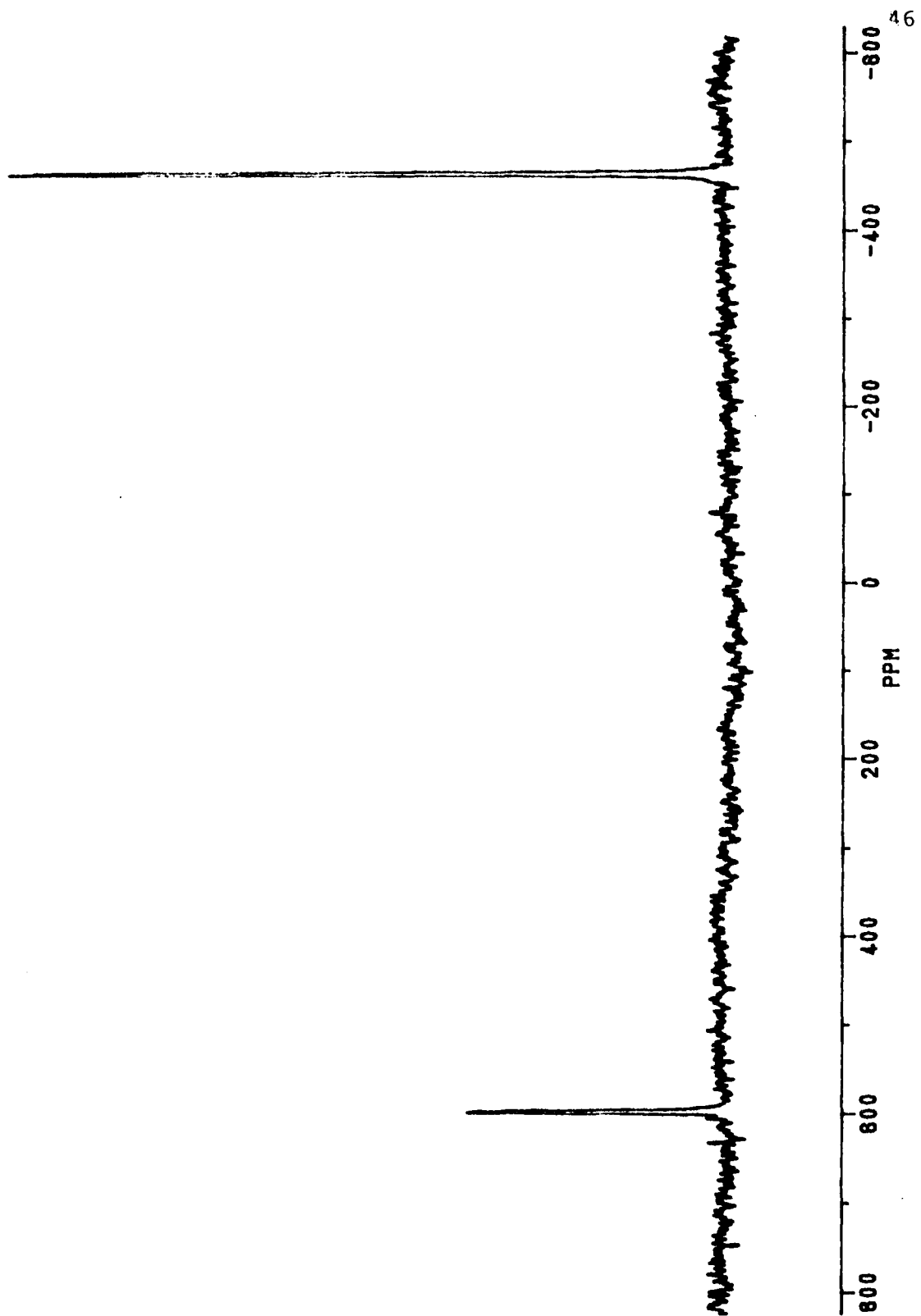
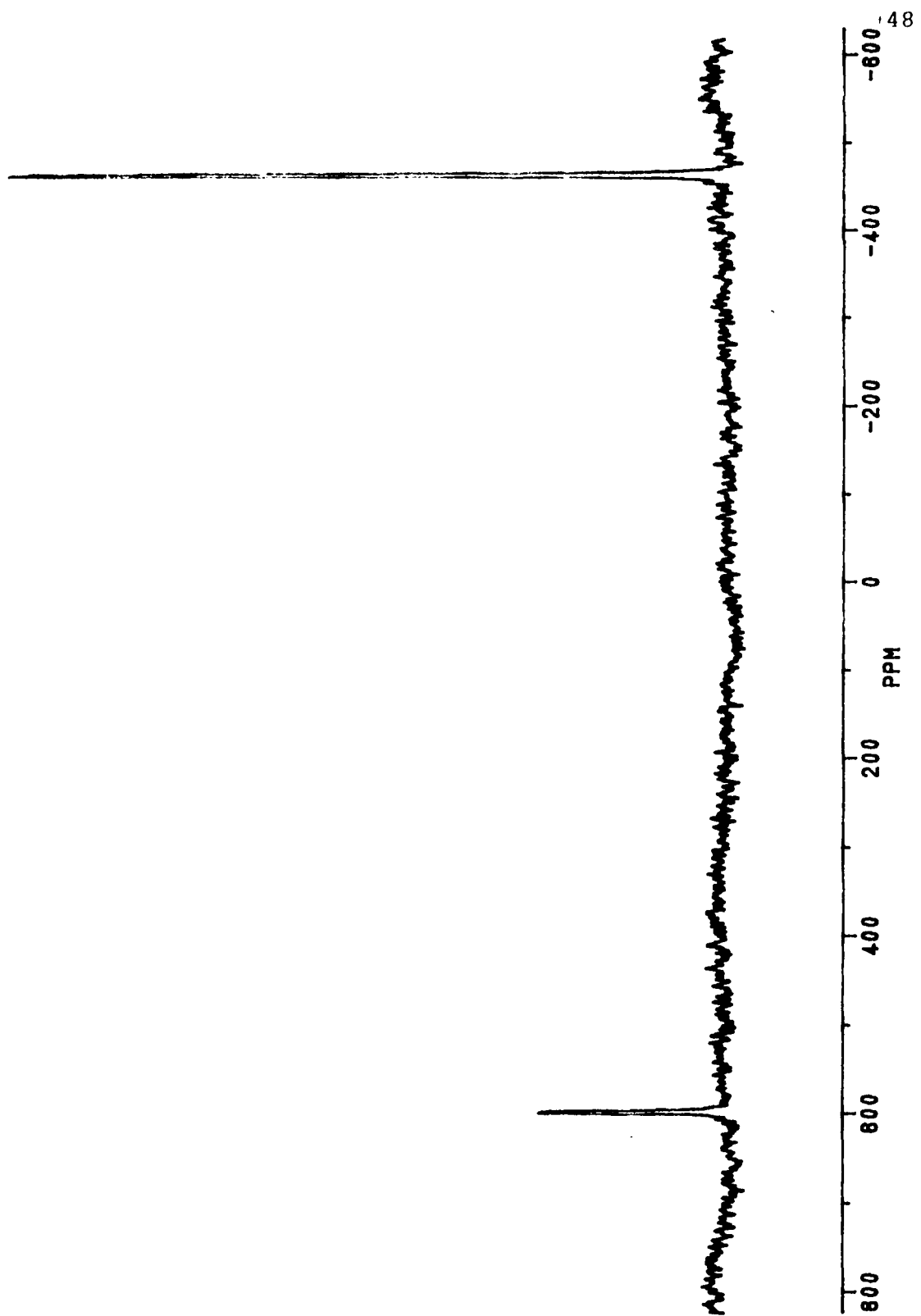


Figure 11. NMR spectrum of solvolysis reaction at 330 K, 229.5 min elapsed time.



temperatures are presented in the appendices.

Once the spectra at this temperature, as well as the other three temperatures, were obtained, they were integrated to yield the ratio of the product to reactant peaks, as discussed in the previous chapter. These ratios were entered into a Microsoft WorksTM spreadsheet and converted to $\ln[\text{reactant}]$. As was also discussed in chapter two, outliers were removed from the data to yield a better correlation coefficient from regression analyses⁶⁰.

The first five data points obtained in the 325 K experiments were removed because no change in ratio was observed. This implies an induction period for the reaction. The data obtained at 335 K and 340 K also had to be manipulated, because the reaction was complete before the end of the measurements. Therefore, several points at the end of these two temperature series were omitted from the linear regression analysis.

The treated data from the first set of experiments are given in Table 1, while the treated data obtained during the duplicated set of experiments are in Table 2.

The $\ln[\text{reactant}]$ data for each temperature of reaction from these tables were plotted as $\ln[\text{reactant}]$ versus time. The spreadsheet had been programmed to calculate a linear regression analysis of the $\ln[\text{reactant}]$ versus time data. A linear regression analysis was applied to each plot and a best fit line was derived from the plotted data points.

Table 1

Natural logarithm of reactant concentration at the different temperatures over 15 time intervals.^a

Elapsed Time (min)	-----ln[reactant]-----			
	325 K	330 K	335 K	340 K
0	0	0	0	0
8.5	---	-4.60×10^{-2}	-9.98×10^{-2}	-1.96×10^{-1}
25.5	---	-1.92×10^{-1}	-1.18×10^{-1}	-2.24×10^{-1}
42.5	---	-2.27×10^{-1}	-1.50×10^{-1}	-4.34×10^{-1}
59.5	---	-2.69×10^{-1}	-4.36×10^{-1}	-7.82×10^{-1}
76.5	---	-2.91×10^{-1}	-4.84×10^{-1}	-1.11
93.5	-8.44×10^{-2}	-3.94×10^{-1}	-7.46×10^{-1}	---
110.5	-9.23×10^{-2}	---	-1.07	-1.32
127.5	-1.11×10^{-1}	-6.50×10^{-1}	-1.21	-1.69
144.5	-1.63×10^{-1}	-6.86×10^{-1}	-1.19	---
161.5	-3.23×10^{-1}	---	-1.48	---
178.5	-3.68×10^{-1}	---	-1.52	---
195.5	-3.82×10^{-1}	-1.08	---	---
212.5	-5.30×10^{-1}	-1.24	---	---
229.5	-5.74×10^{-1}	-1.35	---	---
246.5	-7.30×10^{-1}	-1.30	---	---

a) Outlier omitted from analysis indicated by ---.

Table 2

Natural logarithm of reactant concentration at the different temperatures over 15 time intervals.
(Duplicate Experiments)

Elapsed Time (min)	-----ln[reactant]-----			
	325 K	330 K	335 K	340 K
0	0	0	0	0
8.5	---	-4.59×10^{-2}	-7.97×10^{-2}	-1.72×10^{-1}
25.5	---	---	-1.90×10^{-1}	-2.43×10^{-1}
42.5	---	-1.60×10^{-1}	---	-4.06×10^{-1}
59.5	---	-1.96×10^{-1}	-3.65×10^{-1}	-6.69×10^{-1}
76.5	---	-2.81×10^{-1}	-5.78×10^{-1}	---
93.5	---	-3.82×10^{-1}	-7.08×10^{-1}	-1.14
110.5	-1.42×10^{-1}	-4.27×10^{-1}	---	-1.52
127.5	-2.48×10^{-1}	-5.68×10^{-1}	---	---
144.5	-1.90×10^{-1}	-7.06×10^{-1}	-1.27	-1.66
161.5	-3.07×10^{-1}	-8.14×10^{-1}	-1.24	---
178.5	-3.43×10^{-1}	-1.05	-1.40	---
195.5	-4.91×10^{-1}	-1.13	---	---
212.5	-5.97×10^{-1}	-1.42	---	---
229.5	-6.20×10^{-1}	---	---	---
246.5	-7.93×10^{-1}	---	---	---

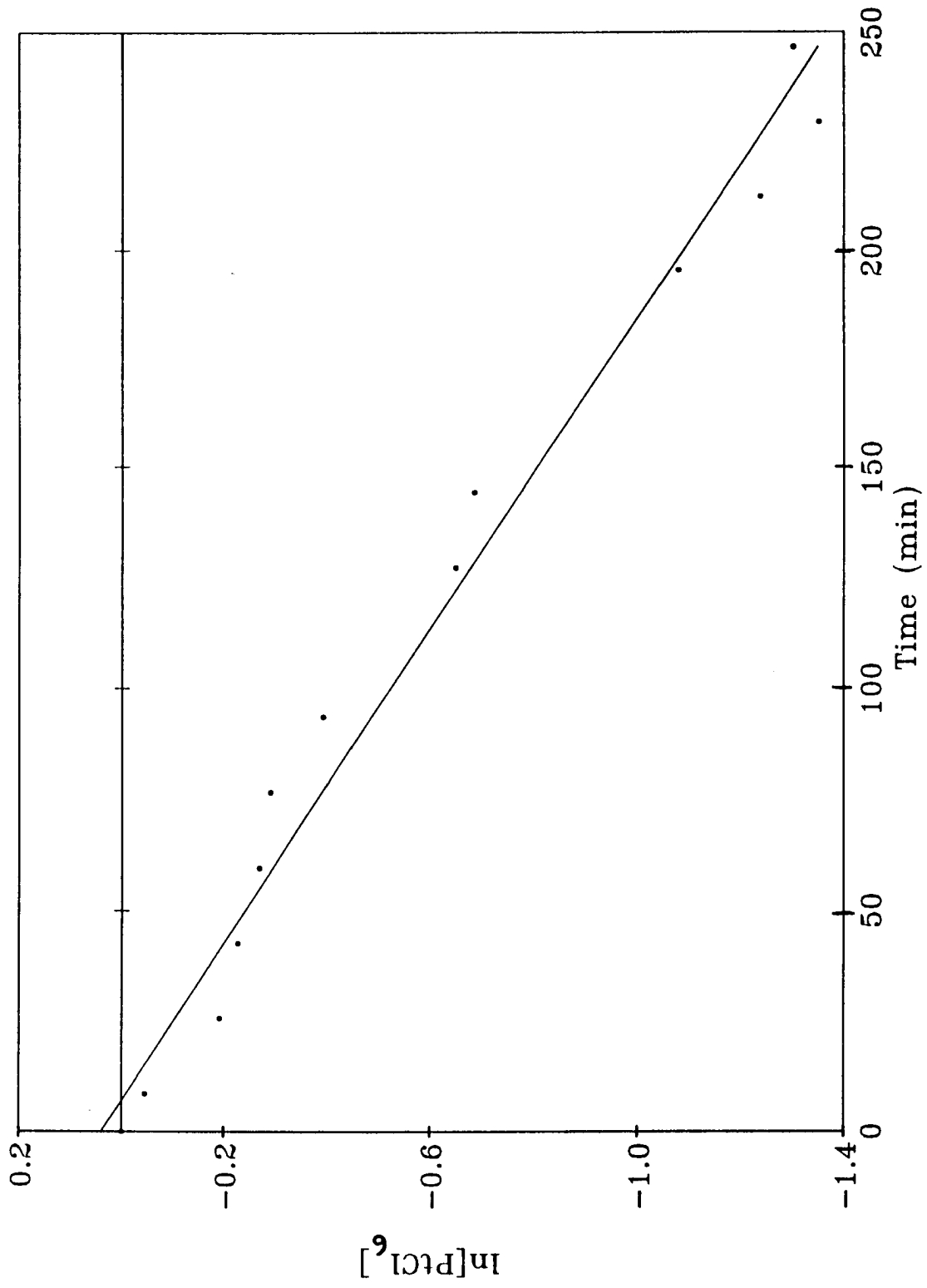
These plots are included in an appendix.

Figure 12 shows the plot of the data for the first experiment performed at 330 K. This plot has a best-fit linear regression line with a correlation coefficient of 0.990 and a slope of $-5.63 \times 10^{-3} \text{ min}^{-1}$. Prior to removal of the outliers, the plot of the data from this experiment had a correlation coefficient of 0.971 and a slope of $-5.74 \times 10^{-3} \text{ min}^{-1}$. The removal of some spurious data points yielded a 1.96% improvement in the correlation coefficient for this experiment at 330 K. The only other experiment in the first series which had outliers removed was the one performed at 340 K. Removal of outliers for this experiment yielded a 2.38% improvement in the correlation coefficient for the best-fit line in the regression analysis. In the duplicate experiments, data point removal resulted in improved correlation coefficients of: 0.93% for 330 K, 4.96% for 335 K, and 3.13% for 340 K.

From first-order kinetics, the slope of the line from a plot of $\ln[\text{reactant}]$ versus time is the negative of the rate constant, k . Pseudo first-order kinetics appear to be in effect here because the correlation coefficient of the best-fit line is nearly unity. Therefore, the slope of this type of plot was used to calculate the k_{obs} for this reaction.

For the first experiment at 330 K the value of the slope was found to be $-5.63 \times 10^{-3} \text{ min}^{-1}$. Therefore the k_{obs} for this experiment is $5.63 \times 10^{-3} \text{ min}^{-1}$ or 9.38×10^{-5}

Figure 12. Plot of $\ln[\text{reactant}]$ versus time for solvolysis reaction at 330 K.



s^{-1} . The second experiment conducted at 330 K yielded a line with a correlation coefficient of 0.979 and a slope of $-6.10 \times 10^{-3} \text{ min}^{-1}$. Therefore the k_{obs} for this experiment is $6.10 \times 10^{-3} \text{ min}^{-1}$ or $1.02 \times 10^{-4} \text{ s}^{-1}$. Taking the mean of these two rate constants yielded an average k_{obs} for 330 K of $5.87 \times 10^{-3} \text{ min}^{-1}$ or $9.78 \times 10^{-5} \text{ s}^{-1}$. The individual rate constants and the average rate constants for this reaction at each temperature, along with the correlation coefficients from the linear regression analyses of the data are given in Table 3.

Now that the temperature dependence of the rate constants for this solvolysis reaction had been determined, the natural logarithms of these values versus the inverse of the temperature was plotted to discern if this reaction obeyed Arrhenius kinetics and to allow the calculation of the activation parameters.

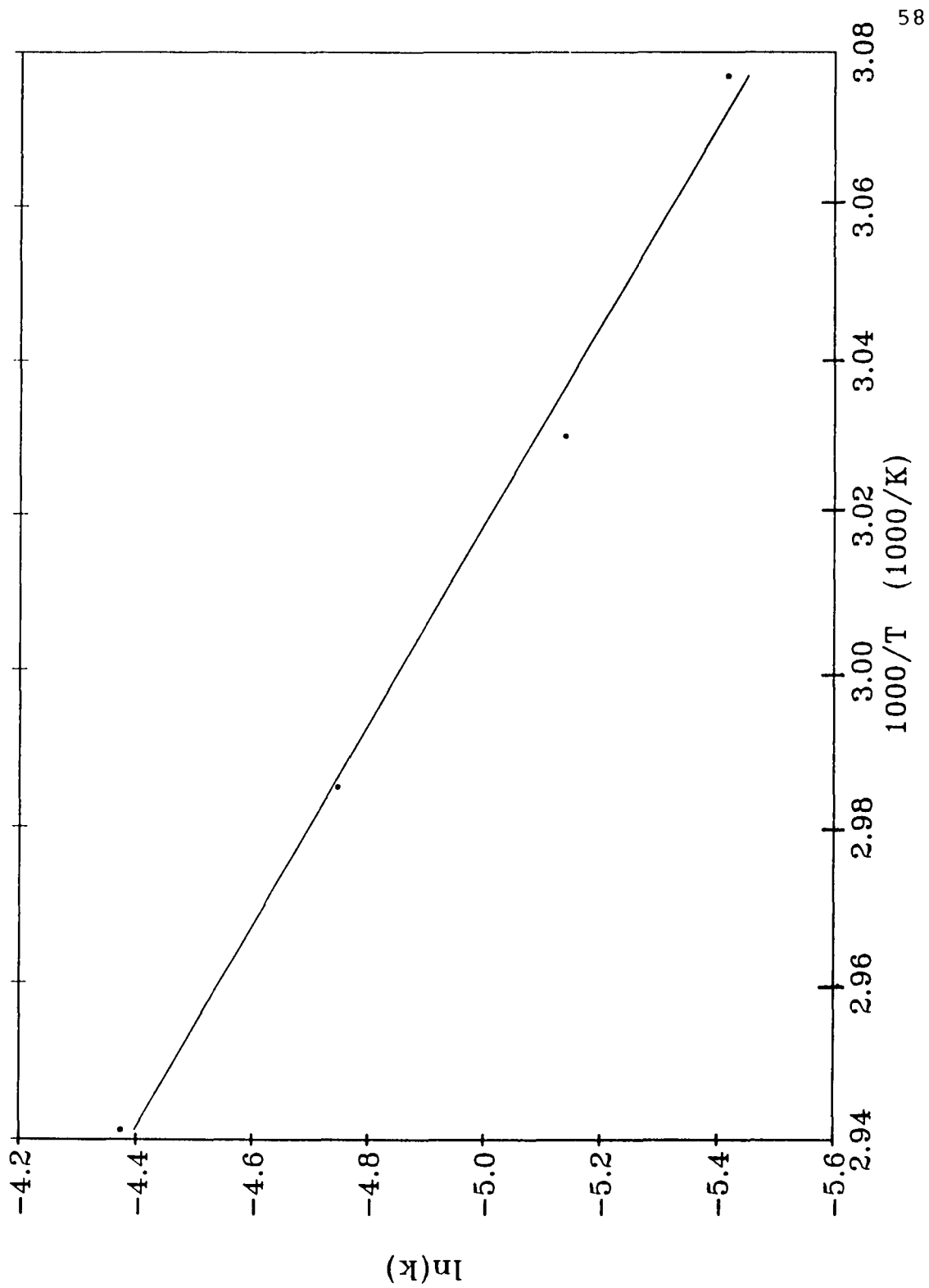
Three plots of $\ln(k_{\text{obs}})$ versus $1000/T$ were made: one for the first set of experiments; one for the second set of experiments; and one using the average values of the rate constants from the different experiments. The plot for the first set of experiments had a correlation coefficient for the best-fit line of 0.994 with a slope of -8.42. The plot for the duplicate set of experiments yielded a correlation coefficient of 0.993 with a slope of -7.05. The plot using the average of the rate constants yielded a correlation coefficient of 0.997 with a slope of -7.76 (Figure 13).

Table 3

Rate constants and statistical data from plots of
 $\ln[\text{reactant}]$ vs. time in variable
 temperature experiments

Temperature/Trial	Rate constant ($\text{min}^{-1}/\text{s}^{-1}$)	Correlation Coeff.
325 K		
Trial 1	$4.27 \times 10^{-3}/7.12 \times 10^{-5}$	0.977
Trial 2	$4.62 \times 10^{-3}/7.70 \times 10^{-5}$	0.971
Average	$4.45 \times 10^{-3}/7.41 \times 10^{-5}$	
330 K		
Trial 1	$5.63 \times 10^{-3}/9.78 \times 10^{-5}$	0.990
Trial 2	$6.10 \times 10^{-3}/1.02 \times 10^{-4}$	0.977
Average	$5.87 \times 10^{-3}/9.78 \times 10^{-5}$	
335 K		
Trial 1	$9.26 \times 10^{-3}/1.54 \times 10^{-4}$	0.985
Trial 2	$8.07 \times 10^{-3}/1.35 \times 10^{-4}$	0.994
Average	$8.67 \times 10^{-3}/1.44 \times 10^{-4}$	
340 K		
Trial 1	$1.29 \times 10^{-2}/2.15 \times 10^{-4}$	0.988
Trial 2	$1.22 \times 10^{-2}/2.03 \times 10^{-4}$	0.988
Average	$1.26 \times 10^{-2}/2.09 \times 10^{-4}$	

Figure 13. Plot of natural logarithm of rate constants versus $1/\text{temperature}$ (Arrhenius Plot).



It was apparent from these plots that this reaction did obey Arrhenius kinetics. Thus, it was possible to calculate various activation parameters for this reaction. The data from the plot of the average of the rate constants were used for these calculations.

From the slope of an Arrhenius plot, it is possible to obtain the activation energy for a chemical reaction. The relationship which yields the activation energy is:

$$\text{slope} = - E_a/R \quad (1)$$

where R is the ideal gas constant. Therefore, the activation energy for the formation of the activated complex in this reaction is given by:

$$E_a = (7.76 \times 10^3 \text{ K}) (8.314 \text{ J K}^{-1} \text{ mol}^{-1})$$

$$E_a = 64.5 \text{ KJ mol}^{-1}$$

The enthalpy of activation, ΔH^\ddagger , is given by the following relationship:

$$\Delta H^\ddagger = E_a - RT \quad (2)$$

Thus, the enthalpy of activation over this temperature range is calculated to be:

$$\Delta H^\ddagger = 64.5 \text{ KJ mol}^{-1} - (8.314 \text{ J K}^{-1} \text{ mol}^{-1}) (332.5 \text{ K})$$

$$\Delta H^\ddagger = 61.7 \text{ KJ mol}^{-1}$$

where 332.5 K is the average of the four temperatures over which the reaction was studied.

The pre-exponential factor, A, in the Arrhenius rate law leads to the calculation of the entropy of activation for a reaction through the following relationship⁵⁹:

$$A = (k_B T e / h) e^{\Delta S^\ddagger / R} (\text{mol dm}^{-3})^{1-n}$$

where k_B is Boltzmann's constant ($1.38 \times 10^{-23} \text{ J K}^{-1}$), e is Euler's number (2.718), and h is Planck's constant ($6.626 \times 10^{-34} \text{ J s}$). The y-intercept for the Arrhenius plot is equal to the natural logarithm of the pre-exponential factor. The y-intercept for the Arrhenius plot of the average rate constants is:

$$\ln(A) = 18.4.$$

Thus,

$$A = 9.80 \times 10^7 \text{ min}^{-1} = 1.63 \times 10^6 \text{ s}^{-1}.$$

Substituting the various constants into the relationship for the entropy of activation yields:

$$\Delta S^\ddagger = (8.314 \text{ J K}^{-1} \text{ mol}^{-1}) \ln \left| \frac{(1.63 \times 10^6 \text{ s}^{-1}) (6.626 \times 10^{-34} \text{ J s})}{(1.38 \times 10^{-23} \text{ J K}^{-1}) (332.5 \text{ K}) (2.718)} \right|$$

Thus,

$$\Delta S^\ddagger = (8.314 \text{ J K}^{-1} \text{ mol}^{-1}) \cdot \ln(8.66 \times 10^{-8})$$

$$\Delta S^\ddagger = -136 \text{ J K}^{-1} \text{ mol}^{-1}.$$

By utilizing the Gibbs-Helmholtz free energy equation the free energy of activation can now be calculated.

$$\Delta G^\ddagger = \Delta H^\ddagger - T\Delta S^\ddagger$$

$$\Delta G^\ddagger = 61.7 \text{ KJ mol}^{-1} - (332.5 \text{ K})(-136 \text{ J K}^{-1} \text{ mol}^{-1})$$

$$\Delta G^\ddagger = 107 \text{ KJ mol}^{-1}.$$

As was stated in the previous chapter, once the kinetic portion of this experiment was concluded, it was time to determine the reversibility of this reaction, thereby allowing calculation of thermodynamic values for this reaction. Spectra obtained for the reaction mixtures which had been used for the kinetic experiments and had been stored for eight weeks, showed that there were still two peaks present, one corresponding to the reactant species and one corresponding to the product species. The ratios were measured and found to be the same for several of the reaction mixtures. Therefore, an equilibrium between the two species had been achieved over time. A concentration equilibrium constant, K_{eq} , could now be calculated as the ratio of the product to reactant concentrations at the conclusion of the reaction at each temperature.

The spectra for the thermodynamic analysis were treated in the same manner as those generated in the kinetic portion

of the experiment. Each peak was integrated to determine the relative areas under the reactant and product species peaks. The ratios of the product to the reactant areas were plotted in the regression analysis spreadsheet previously mentioned, and a temperature dependence for the equilibrium constant was ascertained. The temperature dependence of the equilibrium constant, along with calculations of the free energy of the reaction, allowed for the calculation of the enthalpy and entropy of this solvolysis reaction.

From the long-term, gradual, temperature equilibration experiments described in the previous chapter, four equilibrium constants were discovered; one for each of the temperatures studied. These concentration equilibrium constants were calculated by dividing the ratio of the peaks obtained by the concentration of dimethyl sulfoxide present at the given extent of reaction for each ratio. The initial concentration of DMSO was 4.28 M and the lowest concentration present for these four calculations was 3.50 M. Therefore, DMSO was always present in excess over the hexachloroplatinate(IV).

At $T = 325$ K the K_{eq} was 1.03; at $T = 330$ K the K_{eq} was 0.84; at $T = 335$ K the K_{eq} was 0.64; and at 340 K the K_{eq} was 0.49. From the previously mentioned relationship,

$$\Delta G^{\circ} = -RT \ln(K_{eq}),$$

it is now possible to calculate the free energy change for

this reaction at each temperature. At $T = 325$ K,

$$\Delta G_{325}^{\circ} = -(8.314 \text{ J K}^{-1} \text{ mol}^{-1}) (325 \text{ K}) \ln(1.03)$$

$$\Delta G_{325}^{\circ} = - 0.08 \text{ KJ mol}^{-1} .$$

By similar calculations, $\Delta G_{330}^{\circ} = 0.48 \text{ KJ mol}^{-1}$, $\Delta G_{335}^{\circ} = 1.2 \text{ KJ mol}^{-1}$, and $\Delta G_{340}^{\circ} = 2.0 \text{ KJ mol}^{-1}$. From these values a ΔG° at the average temperature in this range, 332.5 K, was calculated to be,

$$\Delta G_{332.5}^{\circ} = 0.9 \text{ KJ mol}^{-1}.$$

The change in enthalpy for this reaction can be calculated from a plot of $\ln(K_{eq})$ versus $1/\text{temperature}$ by the following relationship⁶¹:

$$d(\ln K)/d(1/T) = - \Delta H^{\circ}/R.$$

A plot of $\ln(K_{eq})$ versus $1/\text{temperature}$ yielded a slope of 5.42×10^3 K, with a correlation coefficient for the best-fit line of 0.997. Therefore, the enthalpy change for this reaction for the average temperature is:

$$\Delta H_{332.5}^{\circ} = -(5.42 \times 10^3 \text{ K}) (8.314 \text{ J K}^{-1} \text{ mol}^{-1})$$

$$\Delta H_{332.5}^{\circ} = -45.1 \text{ KJ mol}^{-1}.$$

Finally, from the Gibbs-Helmholtz equation,

$$\Delta G^{\circ} = \Delta H^{\circ} - T\Delta S^{\circ} ,$$

the entropy change at the average temperature for this reaction, is calculated to be:

$$\Delta S_{332.5}^{\circ} = \frac{-0.9 \text{ KJ mol}^{-1} - 45.1 \text{ KJ mol}^{-1}}{332.5 \text{ K}},$$

thus,

$$\Delta S_{332.5}^{\circ} = -138 \text{ J K}^{-1} \text{ mol}^{-1}.$$

Chapter 4

DISCUSSION AND CONCLUSIONS

As was stated in the introduction of this paper, the major assumption in this study was that the dimethyl sulfoxide molecule would attack the platinum nucleus in the hexachloroplatinate ion displacing a chloride ion. The assumption that only one solvolysis product is formed, is based on the appearance of only one product peak in the spectra and on reports by Elding and Groning⁵⁵ that dimethyl sulfoxide in aqueous solution reacts with tetrachloroplatinate(II) forming a strong, sulfur-bonded 1:1 complex. Goggin and Goodfellow⁹ also attest to the assumption of a single solvolysis product in a study they conducted with tetrachloroplatinate(II) in aqueous dimethyl sulfoxide.

The displacement of the more electronegative chloride with a bulky dimethyl sulfoxide ligand should cause an upfield shift in the NMR spectrum of the platinum nucleus due to a significant shielding effect imparted by the DMSO ligand⁶². Kerrison and Sadler reported on calculations that indicated that the displacement of a chloride ligand by a DMSO ligand will cause an upfield shift of 1000 ppm⁴⁰. When the reaction was run in an NMR tube, a new peak in the spectrum appeared approximately 1000 ppm upfield of the original reactant species peak. It was this anticipated

strong shift in the spectrum that indicated that solvolysis had taken place. From the fact that only one peak was observed, and the information reported by Kerrison and Sadler⁴⁰, it was concluded that it was possible to use NMR to observe the creation of a solvolysis product during this reaction.

Many theories have been developed to explain this upfield shift upon attachment of the DMSO ligand to the platinum nucleus. McFarlane states that attachment of bulky ligands can produce high field shifts due to polarization of the platinum atom⁶³. It is generally believed that the shift to high field upon attachment of a ligand to the platinum nucleus is due to local paramagnetic shielding⁶³⁻⁶⁶. This paramagnetic contribution increases with increasing covalency of the metal to ligand bonds; this increased covalency hinders diamagnetic electron circulation about the platinum nucleus.

If one considers the Pauling electronegativity of Cl ($X_p = 3.16$), S ($X_p = 2.58$), and Pt ($X_p = 2.28$), it will become apparent that the degree of covalency possible in the Pt-S bond is much greater than that found in the Pt-Cl bond due to the closer agreement in electronegativity values for Pt and S. This agrees with the theory about the degree of covalency between the metal and ligand being directly proportional to the increased paramagnetic shielding of the metal nucleus, leading to an upfield shift in the NMR

spectrum. This would seem to explain the phenomena observed during the solvolysis reaction with DMSO.

The kinetic results reported in this study indicate that the solvolysis reaction taking place is very temperature sensitive. Just as one would expect, as the temperature at which the reaction was carried out was increased, a concomitant increase in the rate of reaction was seen. At the lower temperatures, an induction period was observed where virtually no change in reactant concentration occurred for a short time period at the outset of the data acquisition. This induction period was observed to decrease as the temperature at which the reaction was being observed was raised. At the higher temperatures, the reaction was complete before the end of the data acquisition cycle. This phenomenon required that some of the data points near the end of the series be truncated for the kinetic analysis. Once this truncation was performed, the data fit a linear model quite well, assuming the reaction was pseudo-first-order in sodium hexachloroplatinate(IV) hexahydrate concentration.

The assumption that this reaction is pseudo-first-order in sodium hexachloroplatinate(IV) concentration was made based on the fact that any other potential reactants, water and DMSO, were present in excess as solvents. Pseudo first-order kinetics for the solvolysis of potassium tetrachloroplatinate(II) in 5.88 M dimethyl sulfoxide, are reported in

a study conducted by Rund and Palocsay⁶⁷. This information, along with the high correlation coefficients obtained from the first-order plots made from the reaction data obtained, substantiated the assertion that this reaction can be treated as pseudo-first-order in the sodium hexachloroplatinate(IV) concentration.

The average observed rate constants given in Table 3 were: $7.41 \times 10^{-5} \text{ s}^{-1}$ at 325 K, $9.78 \times 10^{-5} \text{ s}^{-1}$ at 330 K, $1.44 \times 10^{-4} \text{ s}^{-1}$ at 335 K, and $2.09 \times 10^{-4} \text{ s}^{-1}$ at 340 K. Groning, Drakenberg and Elding⁵⁴ report some pseudo-first-order rate constants for the solvolysis of $\text{Pt}(\text{H}_2\text{O})_4$ in aqueous dimethyl sulfoxide. The four observed rate constants which they present are: $1.10 \times 10^{-5} \text{ s}^{-1}$ at 298 K, $2.20 \times 10^{-5} \text{ s}^{-1}$ at 303 K, $4.97 \times 10^{-5} \text{ s}^{-1}$ at 310 K, and $9.22 \times 10^{-5} \text{ s}^{-1}$ at 316 K. A similar trend of increasing rate constants with increased temperature is observed for both of these solvolysis reactions. The rate of solvolysis of the platinum-aqua compound appears to be greater than that of the platinum-chloride compound presented in this paper. One potential explanation for this difference could be that the water ligands have no charge to stabilize once they are removed from the complex, whereas the chloride ligands would have a significant charge once they are removed from the complex. Even though a slight difference in the rate constants for these two similar reactions exists, the comparison demonstrates that the values reported in this

paper are reasonable in their order of magnitude.

Once all of the rate constants from both trials at each temperature had been calculated, they were plotted as $\ln(k)$ versus $1/T$ to determine whether the reaction conformed to Arrhenius kinetics. From the three plots which resulted, it was concluded that this reaction did in fact exhibit Arrhenius behavior by virtue of the high correlation coefficients for each plot. This was very gratifying as Arrhenius rate law relationships allow for the calculation of several activation parameters for a reaction. These activation parameters serve to complement both the kinetic information, and the thermodynamic data presented in this paper, and perhaps will be useful to those actively involved in this field of research.

The activation parameters which were calculated include: the activation energy, $E_a = 64.5 \text{ KJ mol}^{-1}$; the enthalpy of activation, $\Delta H^\ddagger = 61.7 \text{ KJ mol}^{-1}$; the entropy of activation, $\Delta S^\ddagger = -136 \text{ J K}^{-1} \text{ mol}^{-1}$; and the free energy of activation, $\Delta G^\ddagger = 107 \text{ KJ mol}^{-1}$. An Arrhenius plot was made for the rate constants of the solvolysis of the platinum-aqua compound previously discussed, and the following activation parameters were calculated⁵⁴: $E_a = 93 \text{ KJ mol}^{-1}$; $\Delta H^\ddagger = 90 \text{ KJ mol}^{-1}$; $\Delta S^\ddagger = 2 \text{ J K}^{-1} \text{ mol}^{-1}$; and $\Delta G^\ddagger = 89 \text{ KJ mol}^{-1}$. While both of these reactions show similar values for most of their thermodynamic activation parameters, they vary significantly in their entropies of activation.

Groning, Drakenberg and Elding suggest that the positive ΔS° value indicates that a dissociative process is occurring in the creation of the activated complex. This would suggest that an associative process is occurring for the formation of the activated complex for the solvolysis of the hexachloroplatinate(IV) in DMSO.

The thermodynamic data presented in this paper illustrates that, once the proper activation barrier has been overcome, this reaction proceeds to products in an exothermic manner. It was also evident that an equilibrium situation is established which allows both reactant and product species to coexist in different ratios depending upon the temperature of observation. It is apparent from the ΔG° values that the product species is more thermodynamically stable at lower temperatures as these ΔG° values increased with increasing temperature.

The change in enthalpy for this reaction favors the products, while the change in entropy of this reaction favors the reactants. This decrease in the measure of disorder in the system may be due to the larger dimethyl sulfoxide ligands replacing the small chloride ligands in the reactant species, thereby limiting the degrees of freedom of the platinum complex. This decrease in the entropy of the system is large enough to outweigh the favorable enthalpy factor leading to an overall unfavorable change in the free energy of the reaction over the

temperature range studied. In a study previously mentioned, Elding and Groning⁵⁵ give thermodynamic values for the acid hydrolysis of some platinum-chloro compounds. The data given in their study indicate similar findings, the free energy changes for reactions of this type are unfavorable over the temperature range studied. One possibility for the increase in the free energy in both of these chloride anations, is that the greater difference in electronegativity between the chloride and platinum, versus sulfur and platinum, yields a bond which is more stable than the one being formed.

While the kinetic experiments were being conducted, small needlelike crystals were observed forming at the bottom of some of the NMR tubes after they had been removed from the magnet and allowed to stand at room temperature for several days. When a pipet was inserted to remove the supernatant in order to isolate a crystal for x-ray crystallographic analysis, a cloudy, white precipitate immediately developed. The samples were evidently supersaturated with the solvolysis product and required only minor agitation to cause precipitation of the product.

The tubes were washed several times with distilled H₂O and samples of this precipitate were gathered. The precipitate was placed into a freeze drying unit to remove the remaining moisture and then transferred to a desiccator for storage.

Future study on this topic will be centered around identifying the exact composition and structure of this solvolysis product. Identification of the compound along with the kinetic and thermodynamic data presented in this paper might lead to the discovery of the mechanism of this reaction.

One hypothesis as to the identity of this precipitate is that it is an insoluble hydroxide formed from further reaction of the solvolysis product with the water present in the NMR tube. The solvolysis of the sodium hexachloroplatinate(IV) by dimethyl sulfoxide, studied here, might be the initial step(s) in the production of an insoluble platinum hydroxide. Rund and Palocsay⁶⁷ report on a study where DMSO solvolyzes tetrachloroplatinate(II) through a series of relatively fast pseudo-first-order reactions, producing a labile intermediate which then proceeds to react with 1,10-phenanthroline to form the final product. The reason that the precipitate is not seen during the solvolysis reaction is possibly due to the fact that DMSO is much more efficient than water as an entering ligand when chloride is the leaving group; 4.4×10^3 times faster⁵⁴.

Further study of this precipitate could be done by atomic absorption analysis, mass spectrometry, infra-red absorption analysis or an appropriate organic solvent could be chosen to dissolve the precipitate allowing nuclear magnetic resonance spectroscopy to be performed to yield

information about composition and structure. These techniques were not employed here as the focus of this study was on the use of platinum-195 nuclear magnetic resonance spectroscopy to investigate a solvolysis reaction.

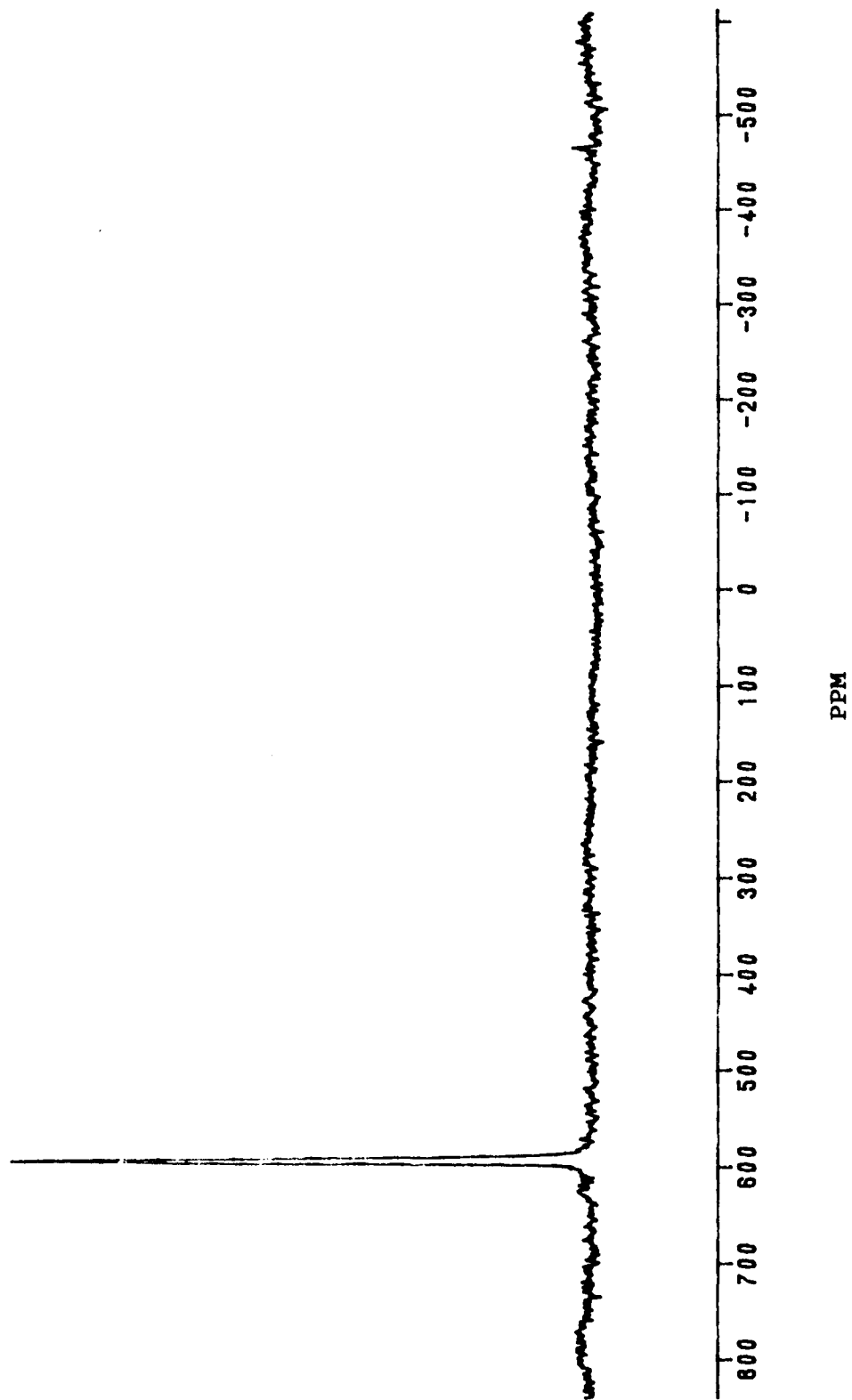
Future study of this topic might be done by coordination chemists who would be interested in the process of ligand approach and the theoretical construction of any intermediates through which the reaction coordinate proceeds. Further kinetic and thermodynamic studies on this type of reaction could be conducted with different platinum compounds to establish more parameters which might assist in the development of better chemotherapeutic agents. The temperature range over which this study was conducted could be enlarged to look for any anomalous behavior of this reaction as a function of temperature. The major challenge of increasing the temperature would be measuring the reaction accurately as it begins to occur rapidly at 340 K. One would expect this trend of acceleration to continue beyond 340 K.

This research project has supplied some much needed information about the reactivity of the platinum nucleus. It is this author's sincere hope that the information discovered during this study will benefit the scientific and medical communities in their ongoing efforts to defeat cancer.

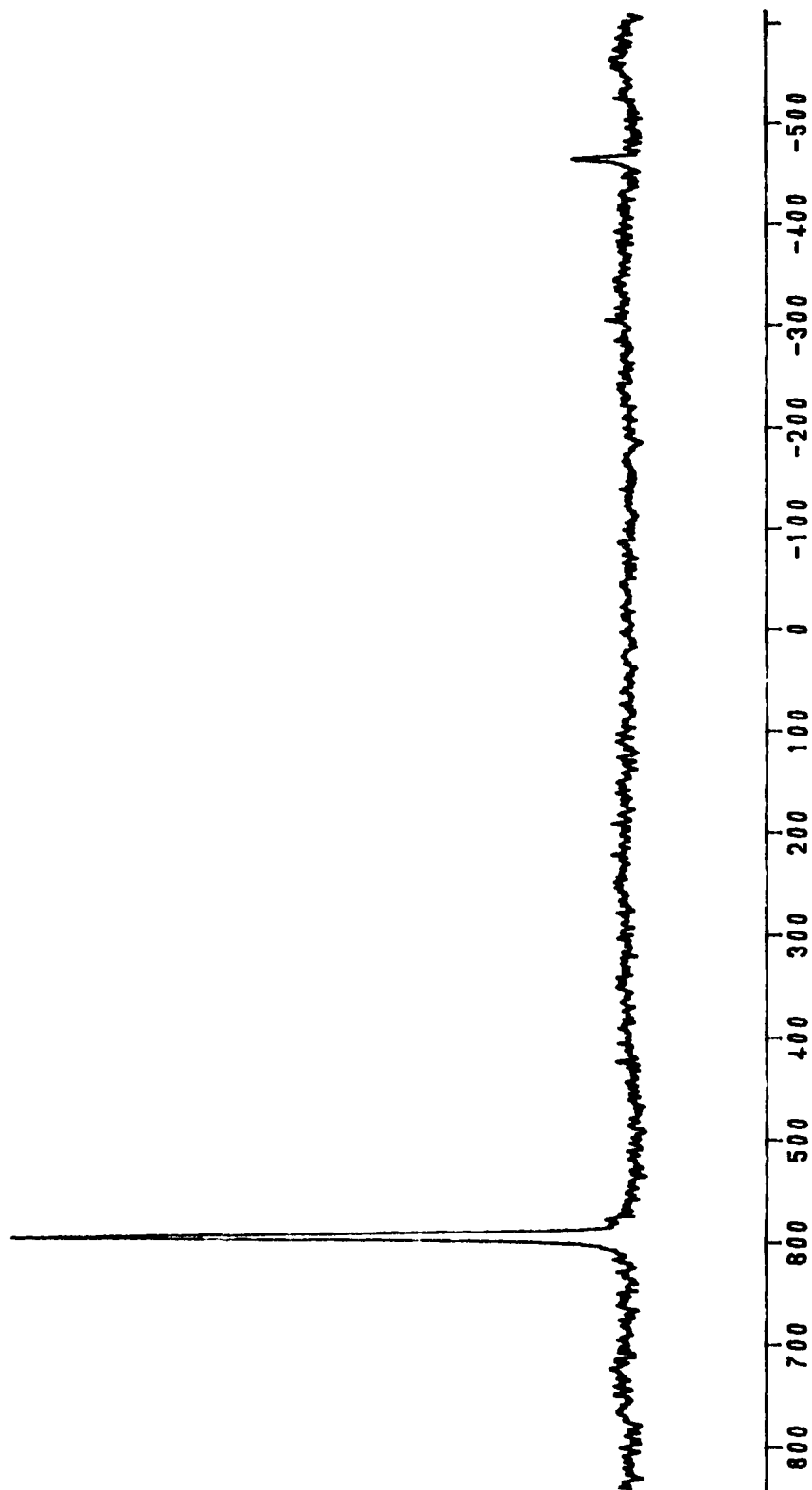
APPENDICES

APPENDIX I

T = 325 K, 8.5 min

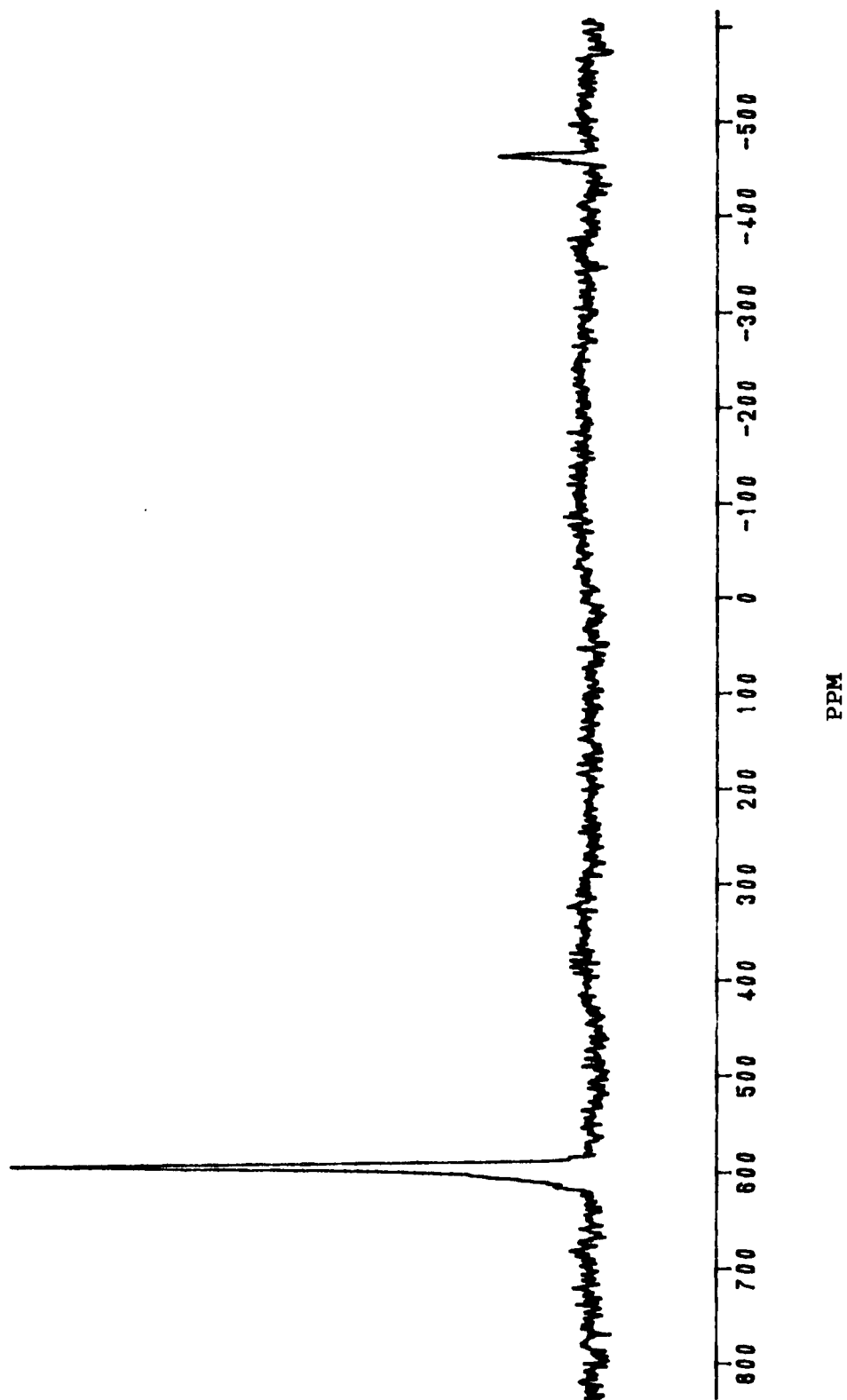


T = 325 K, 42.5 min

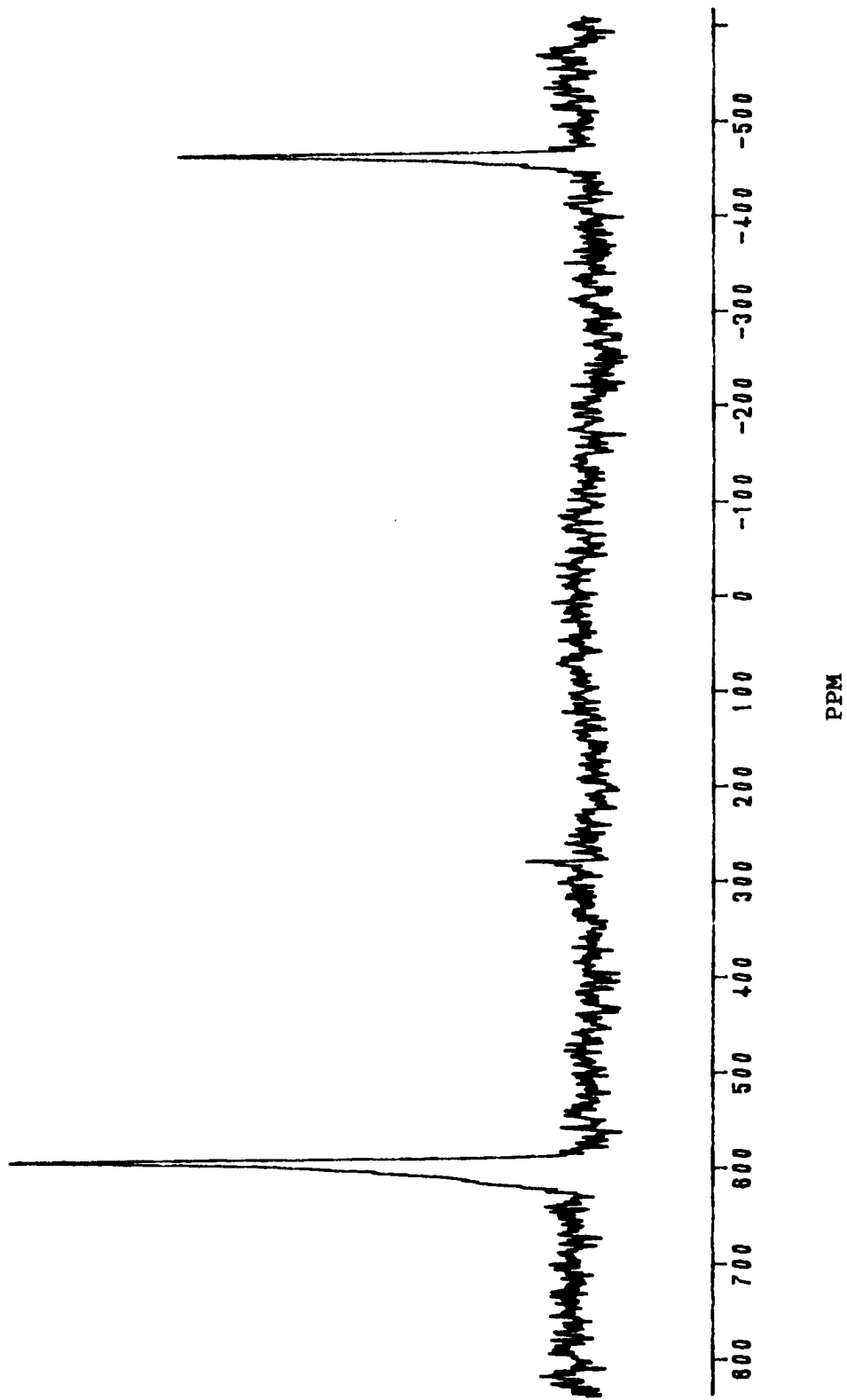


PPM

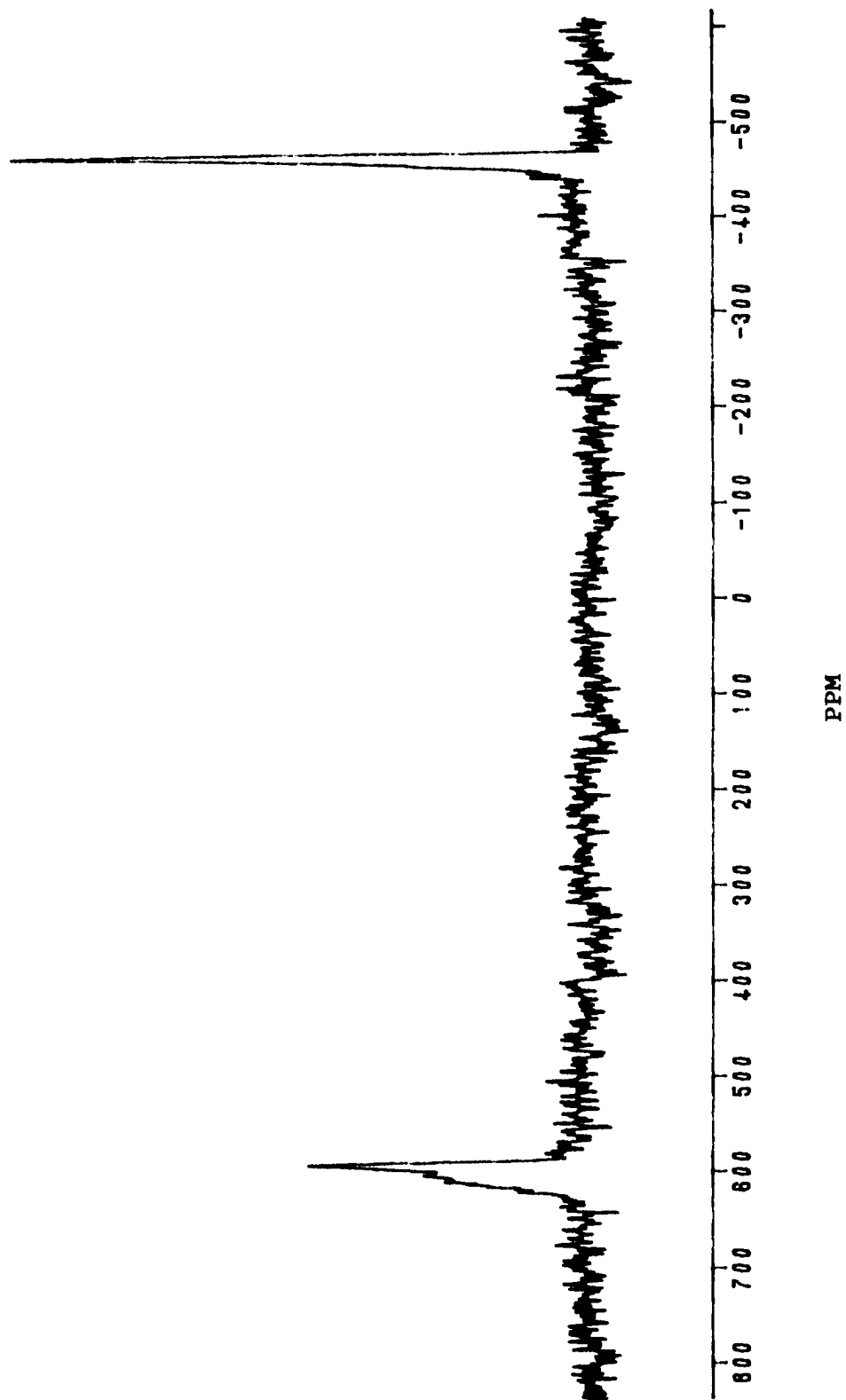
T = 325 K, 93.5 min



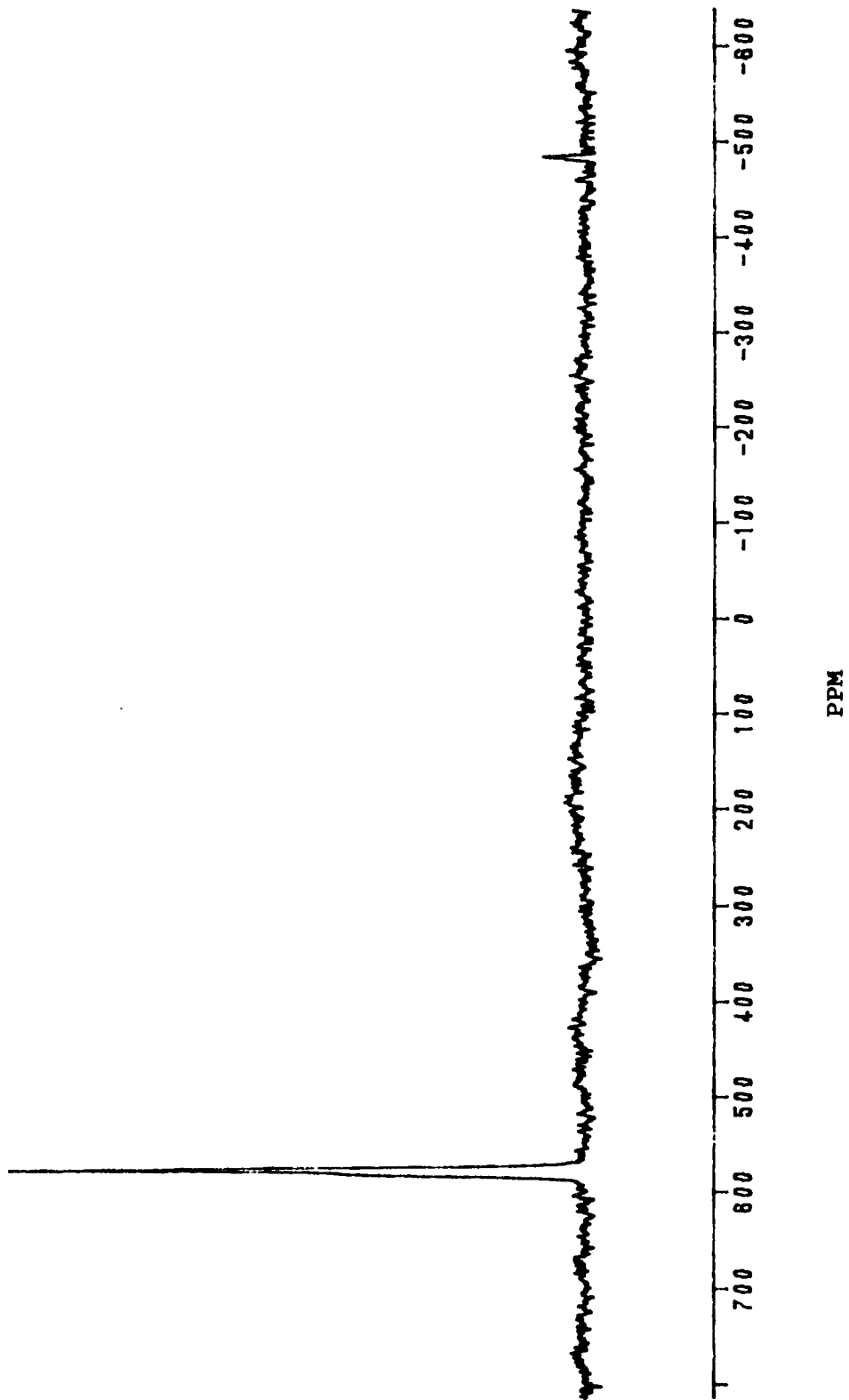
T = 325 K, 178.5 min



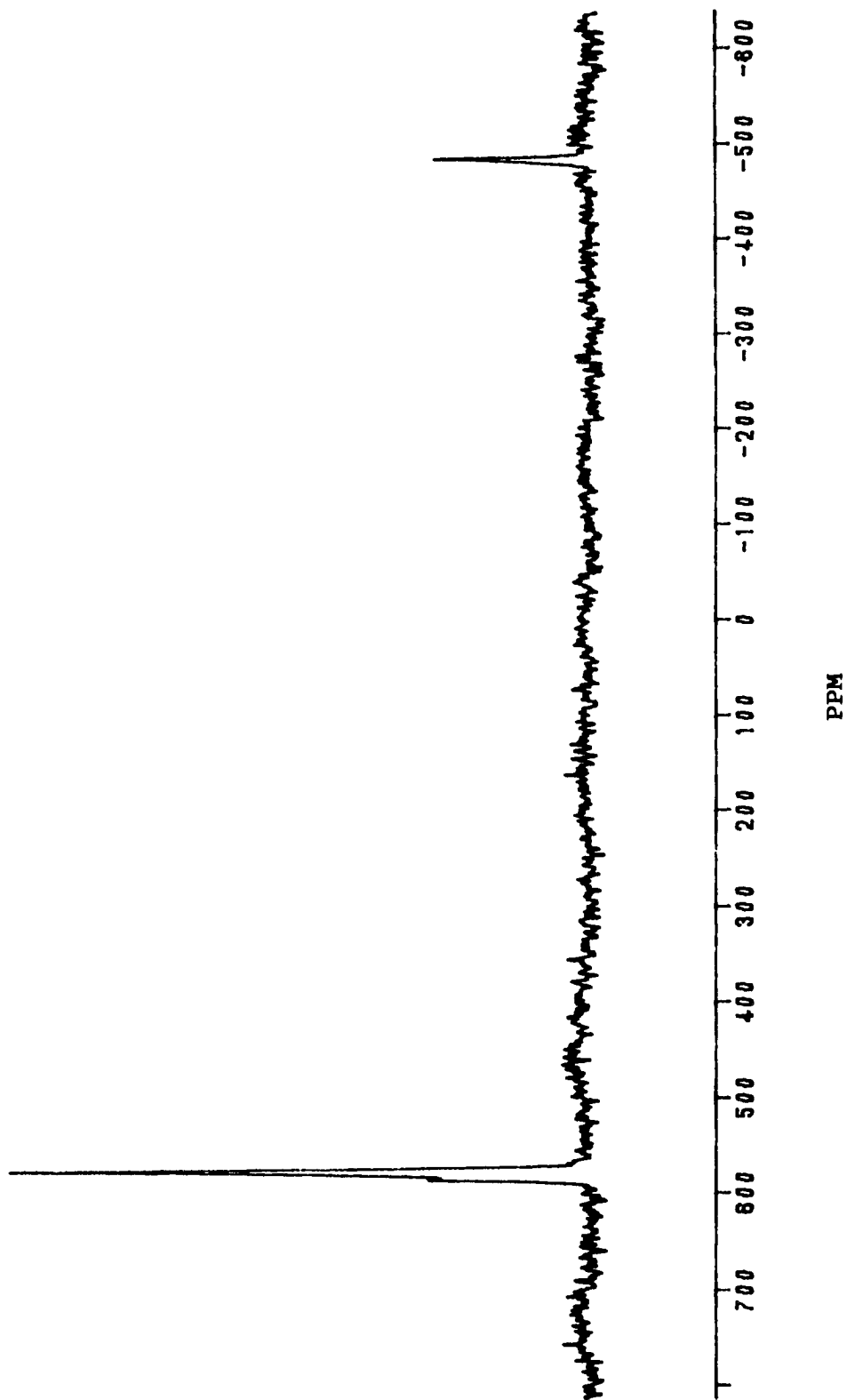
T = 325 K, 246.5 min



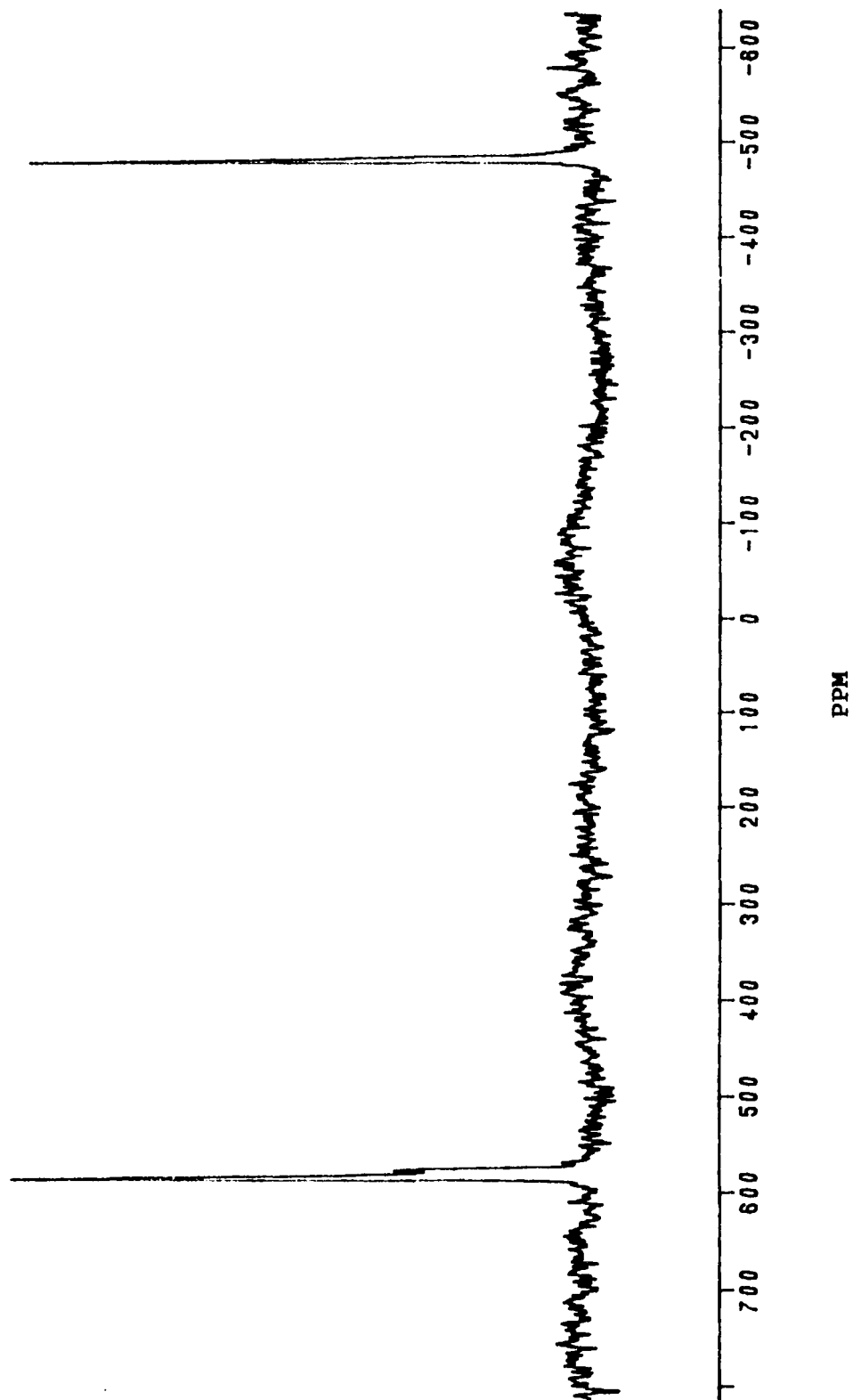
T = 335 K, 8.5 min



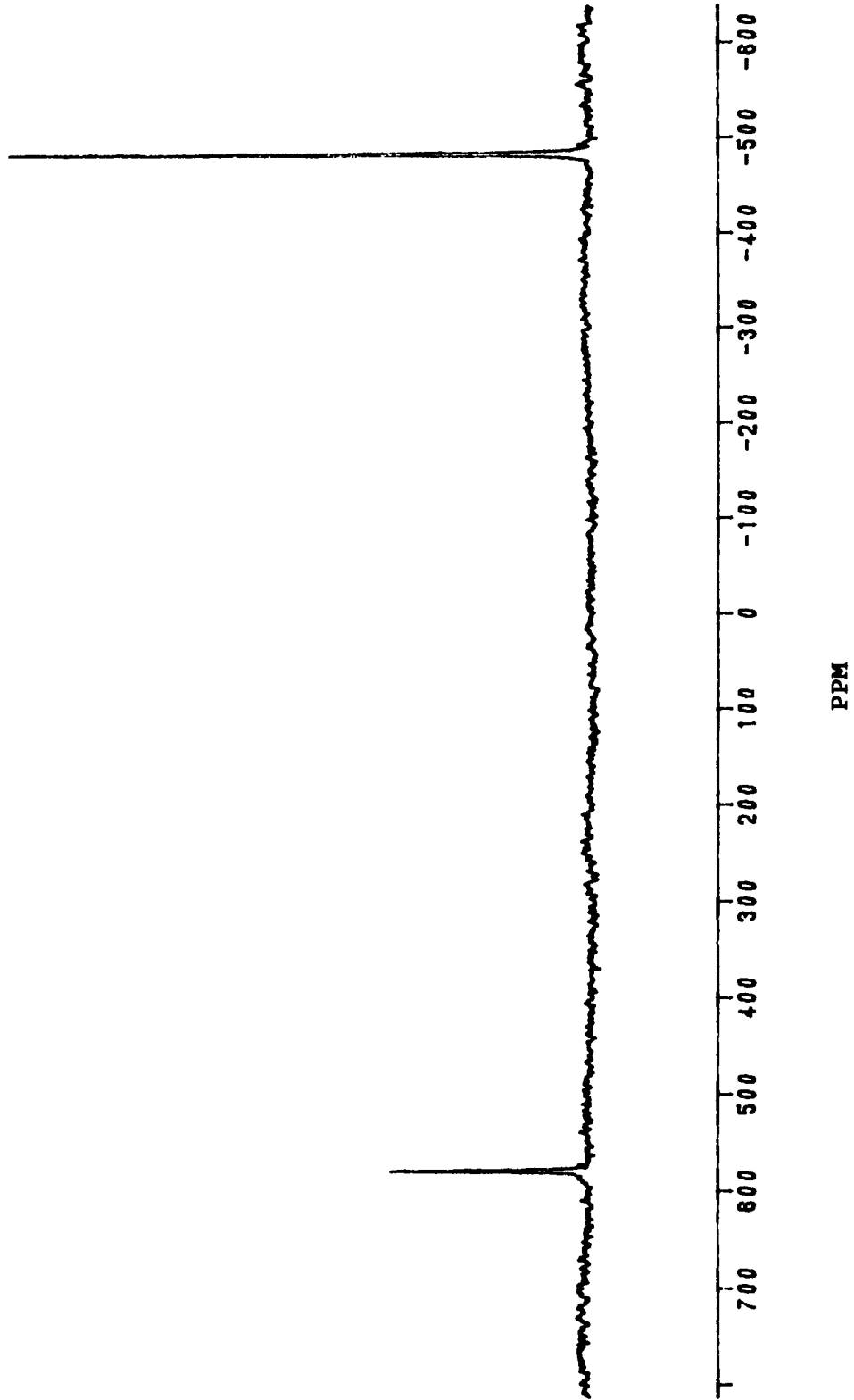
T = 335 K, 42.5 min



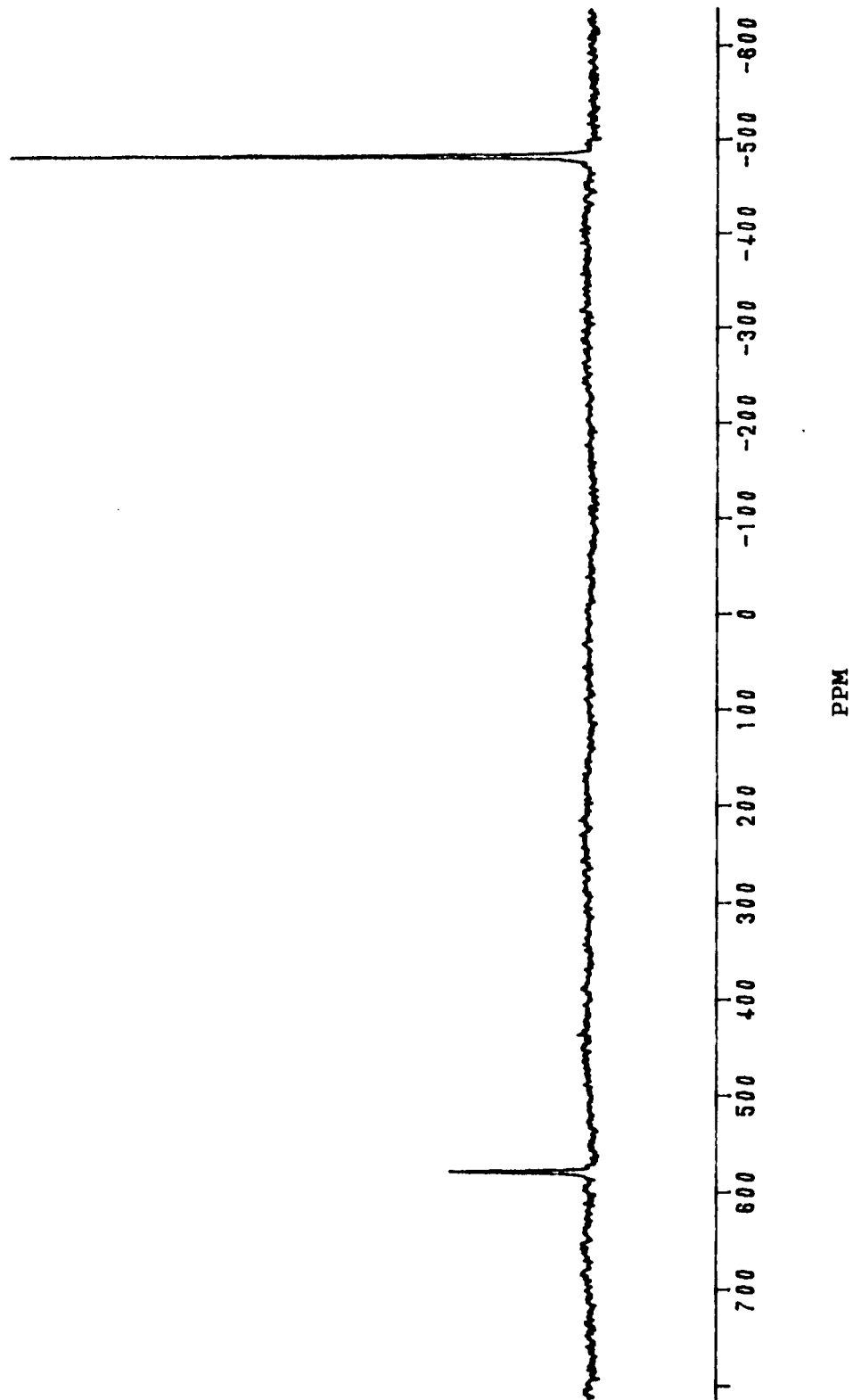
T = 335 K, 76.5 min



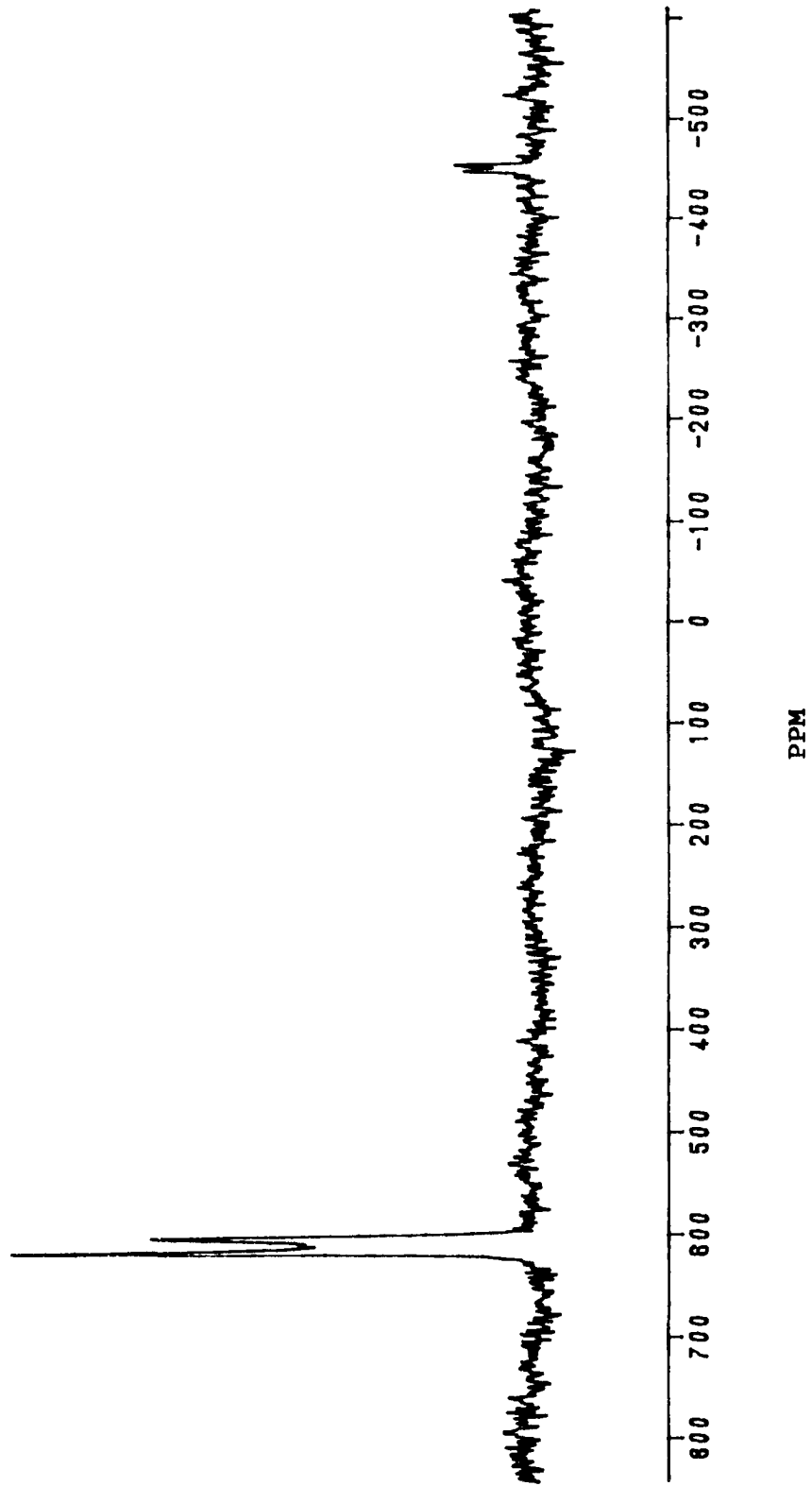
T = 335 K, 110.5 min



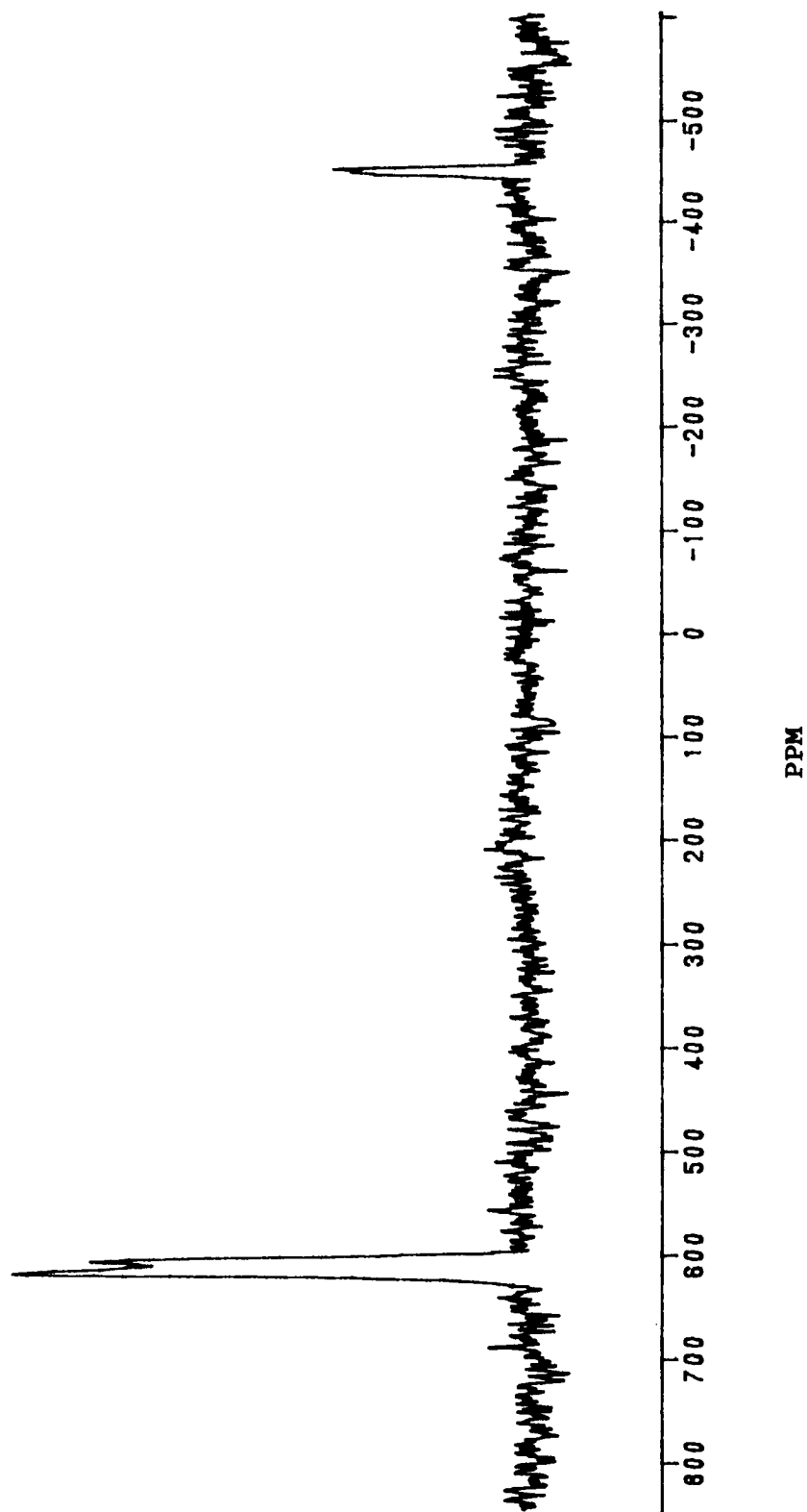
T = 335 K, 161.5 min



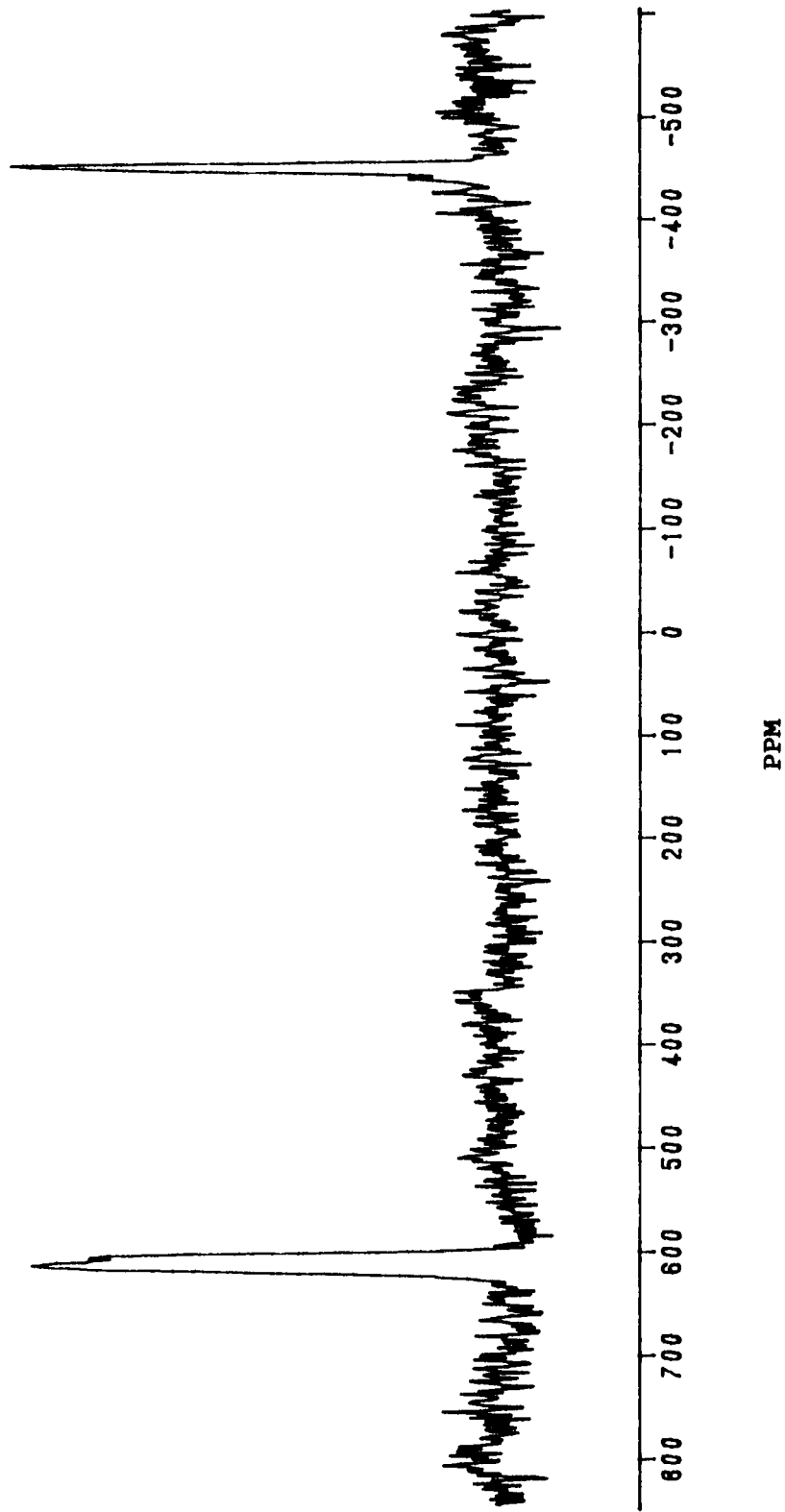
T = 340 K, 8.5 min



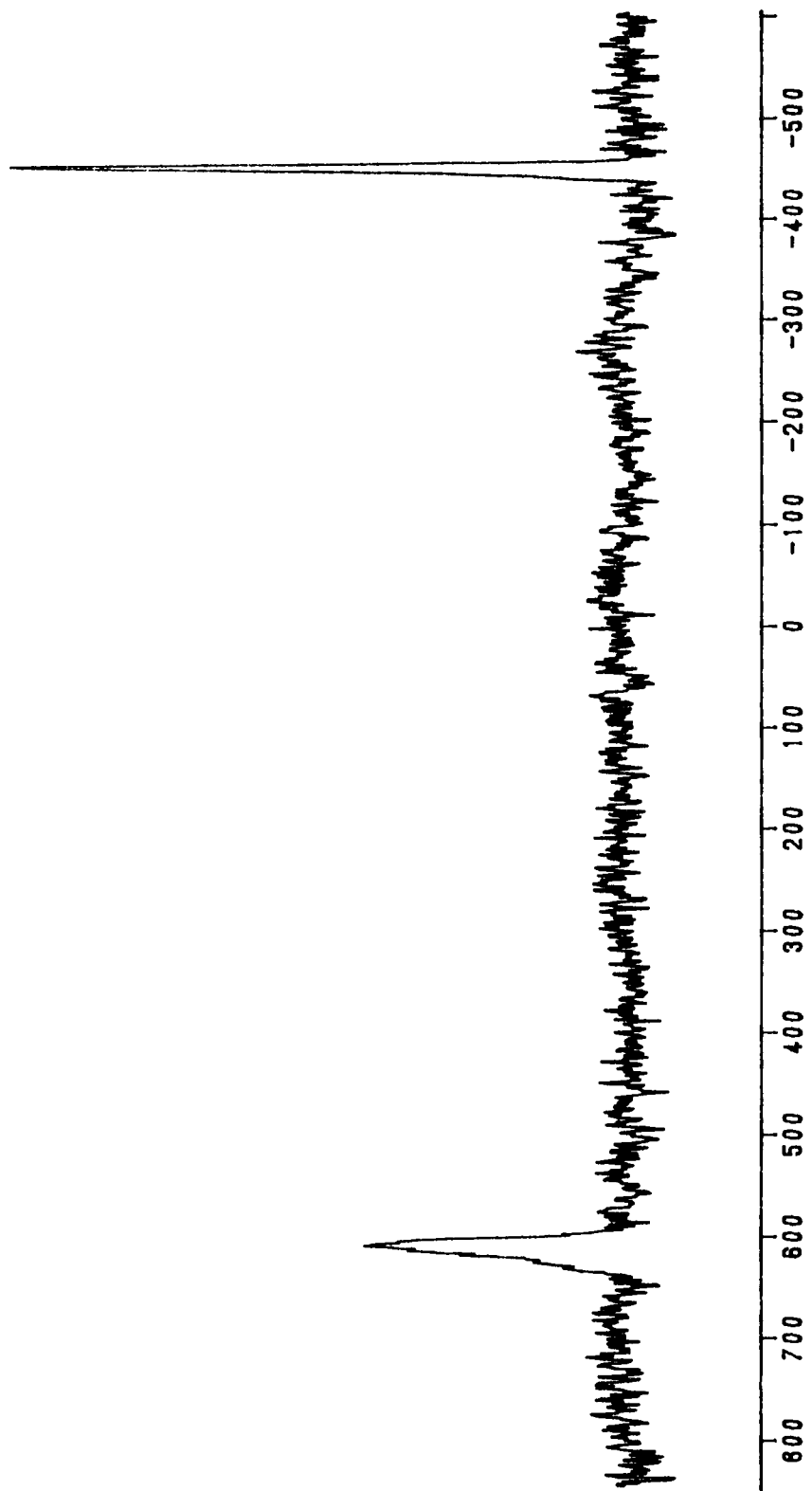
T = 340 K, 25.5 min



T = 340 K, 42.5 min

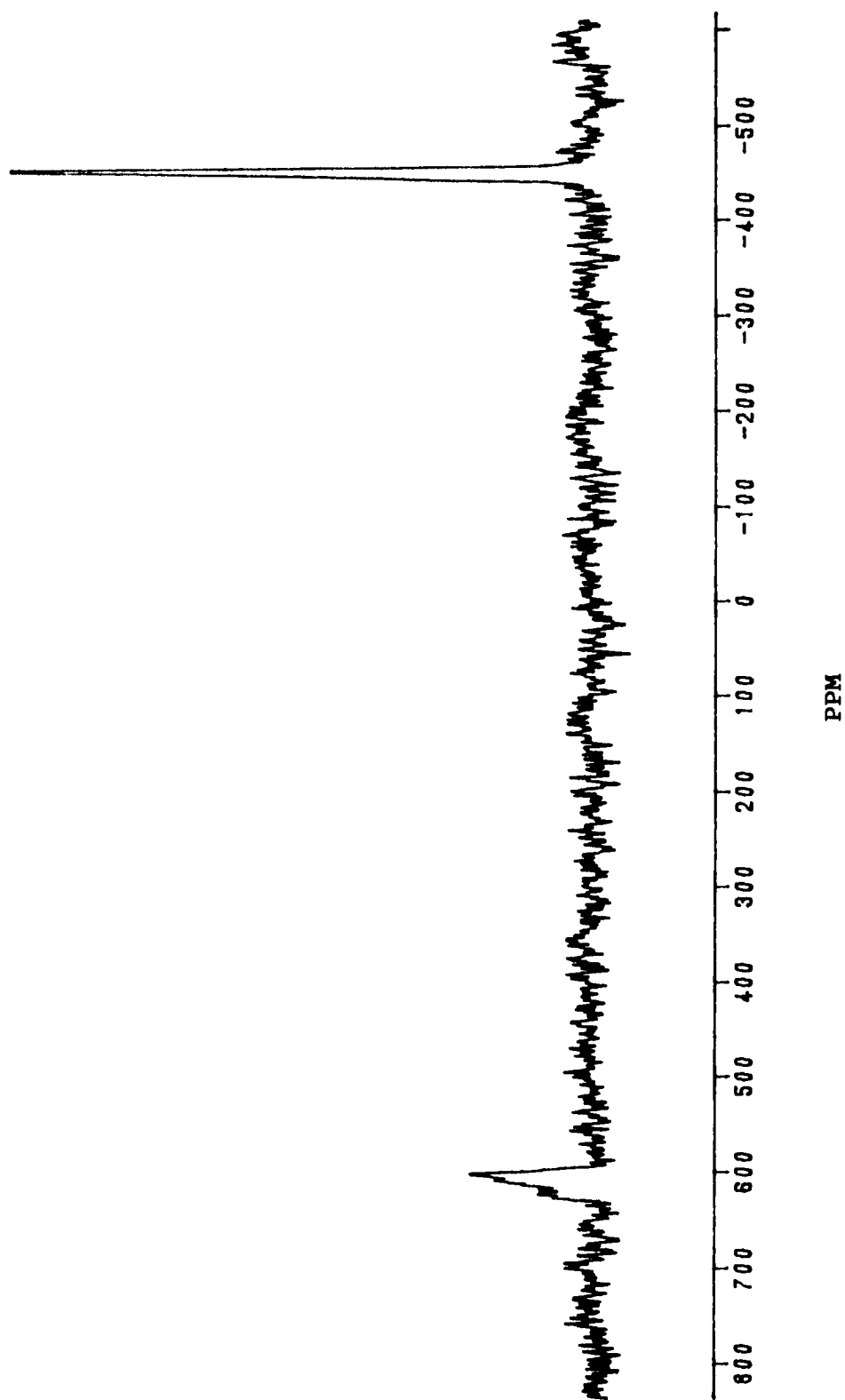


T = 340 K, 59.5 min

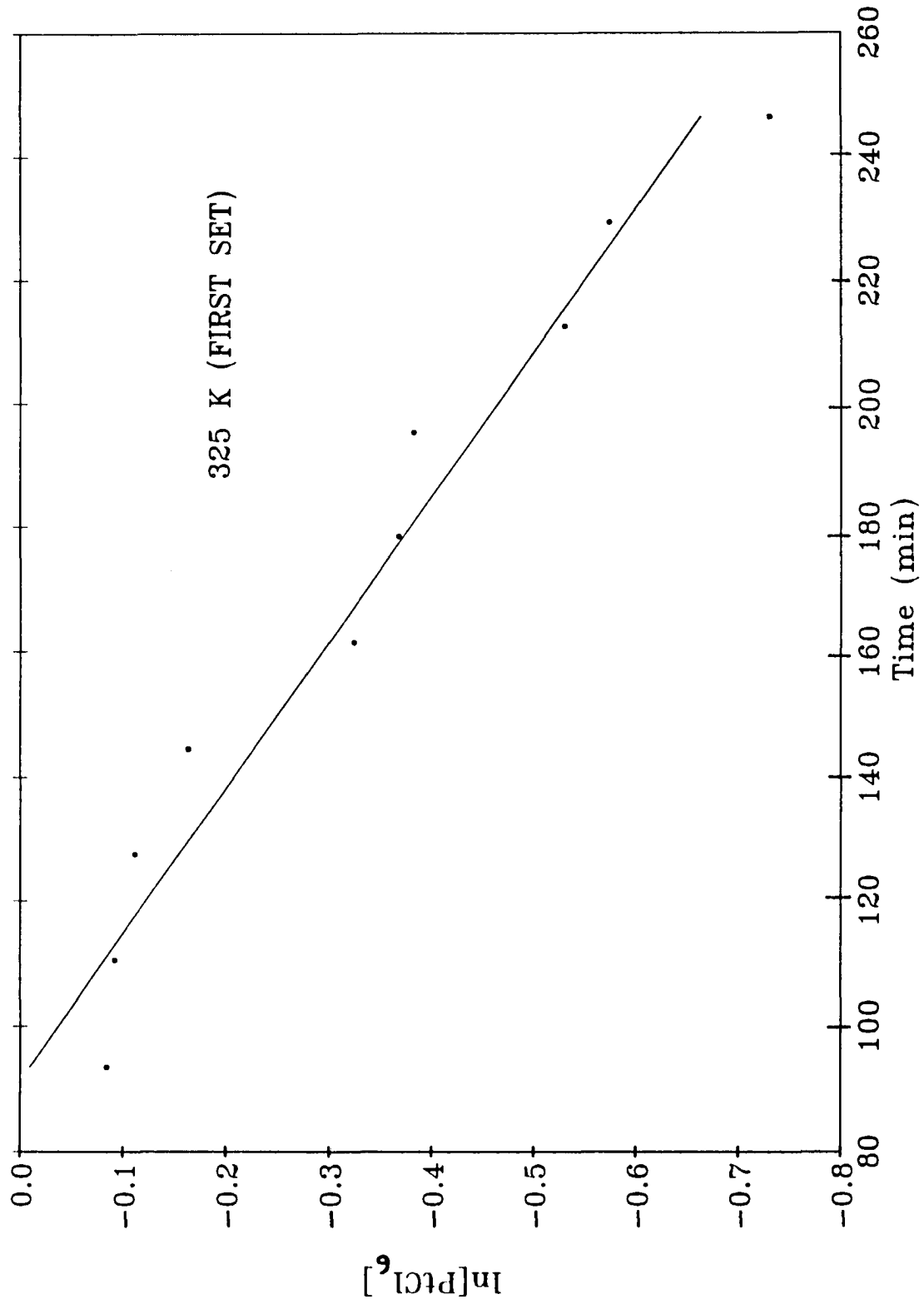


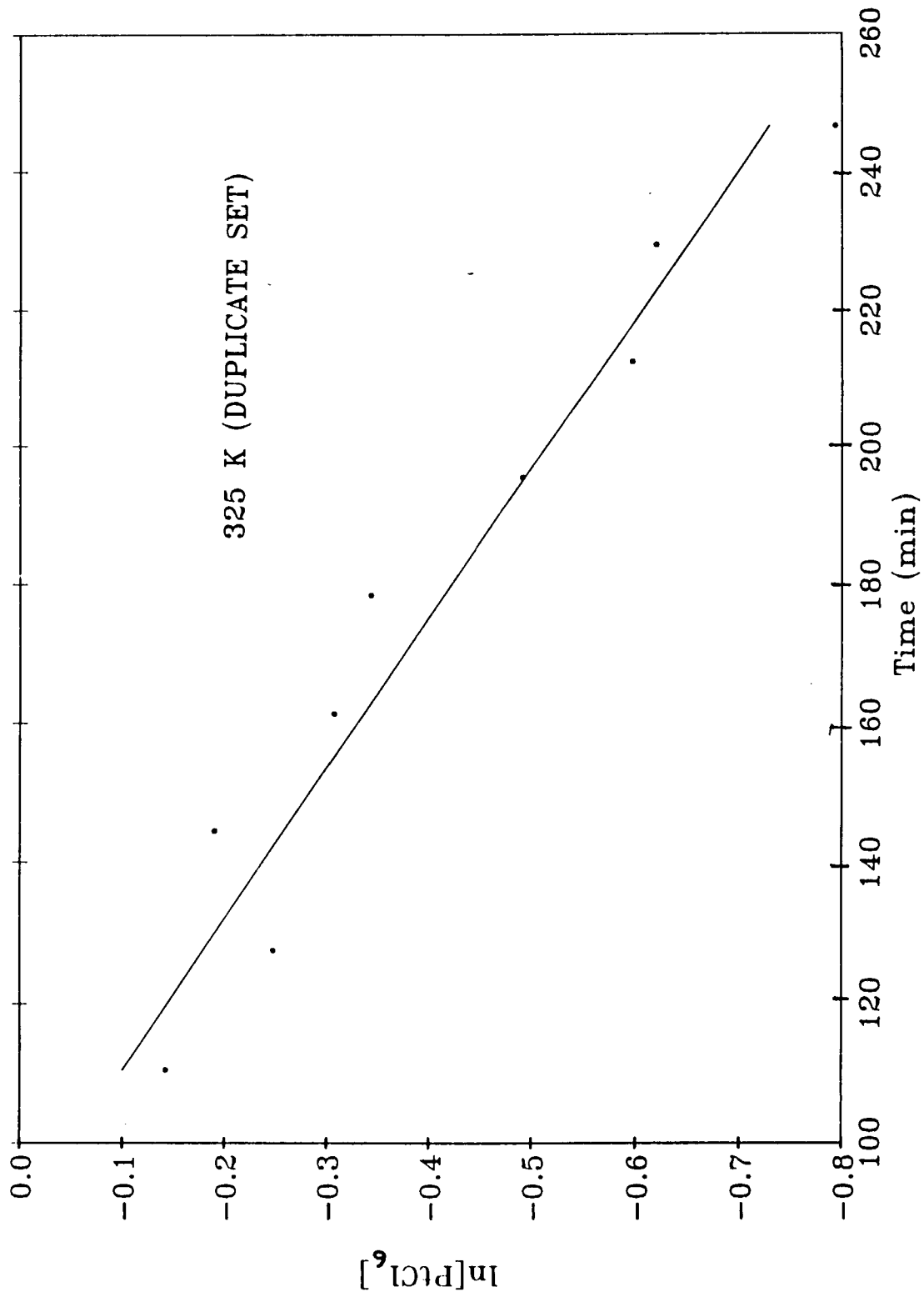
PPM

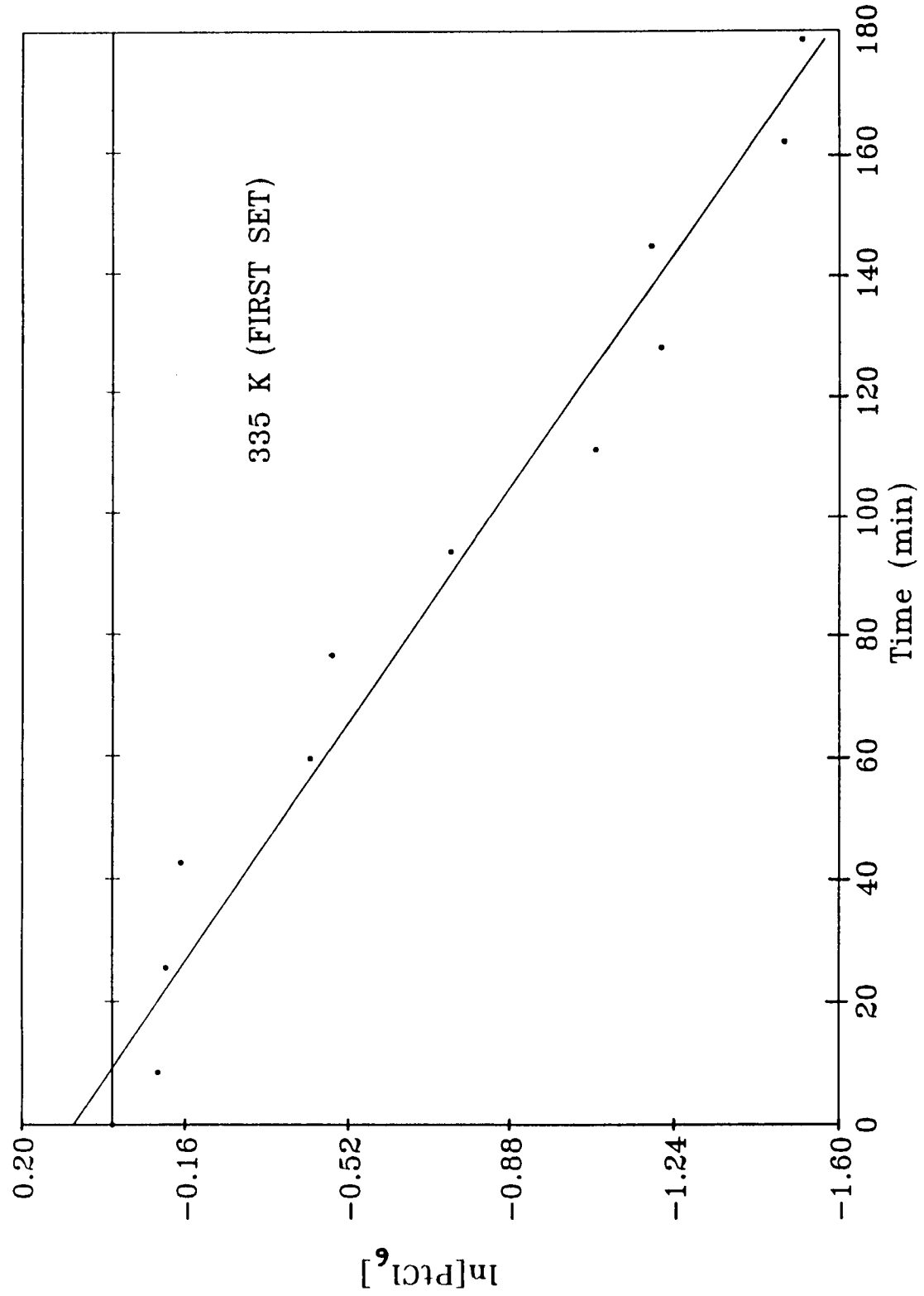
T = 340 K, 76.5 min

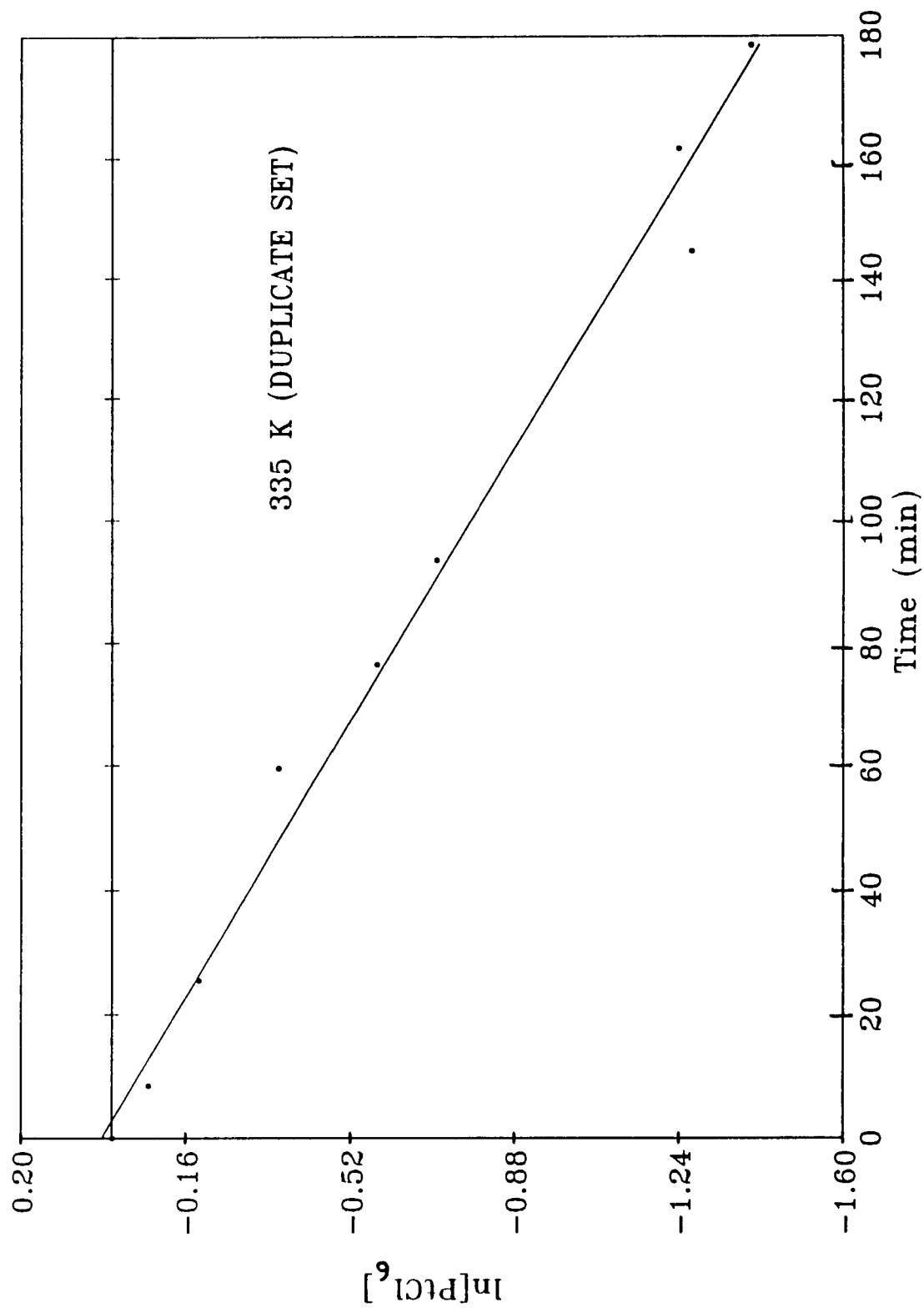


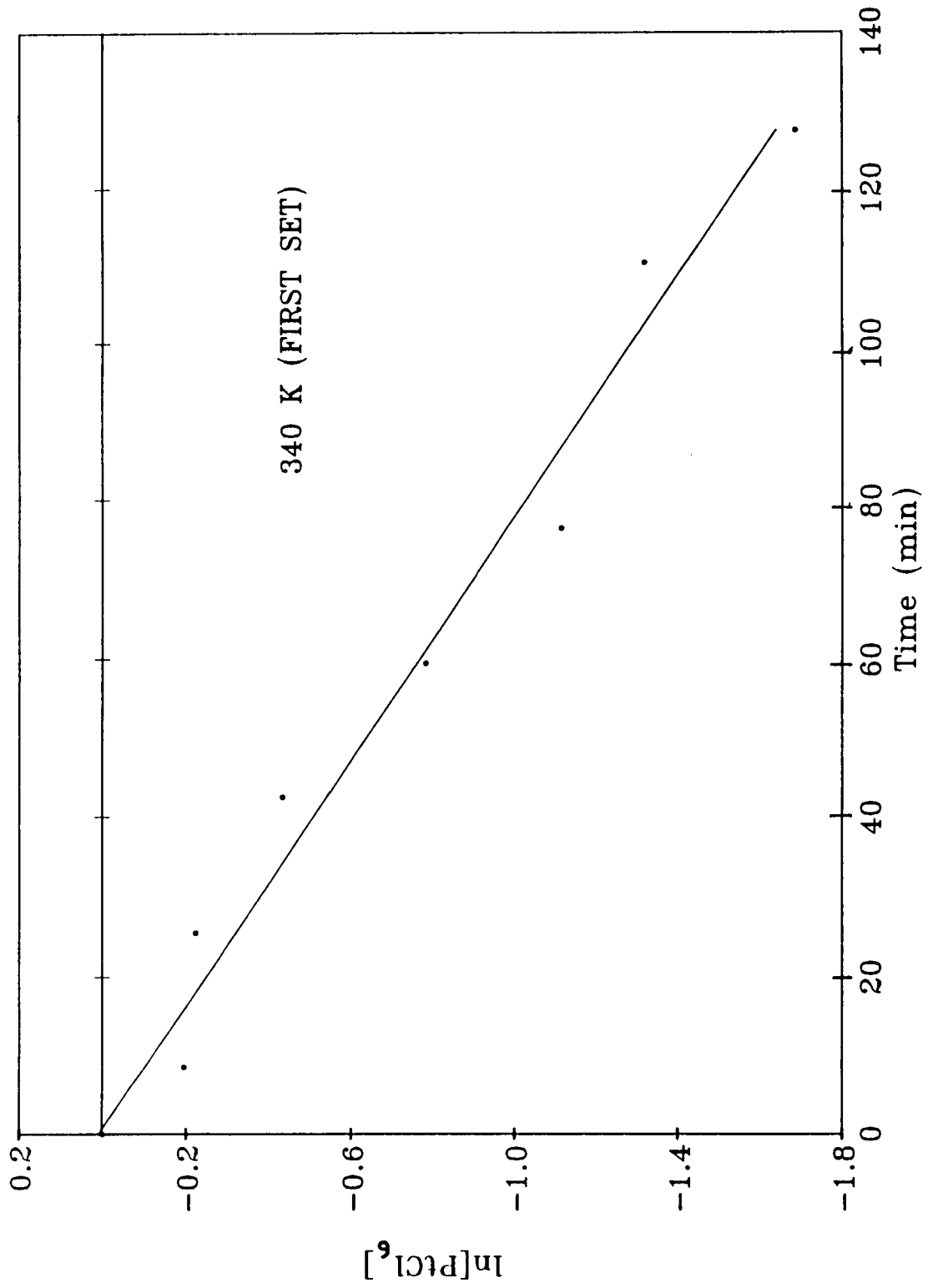
APPENDIX II

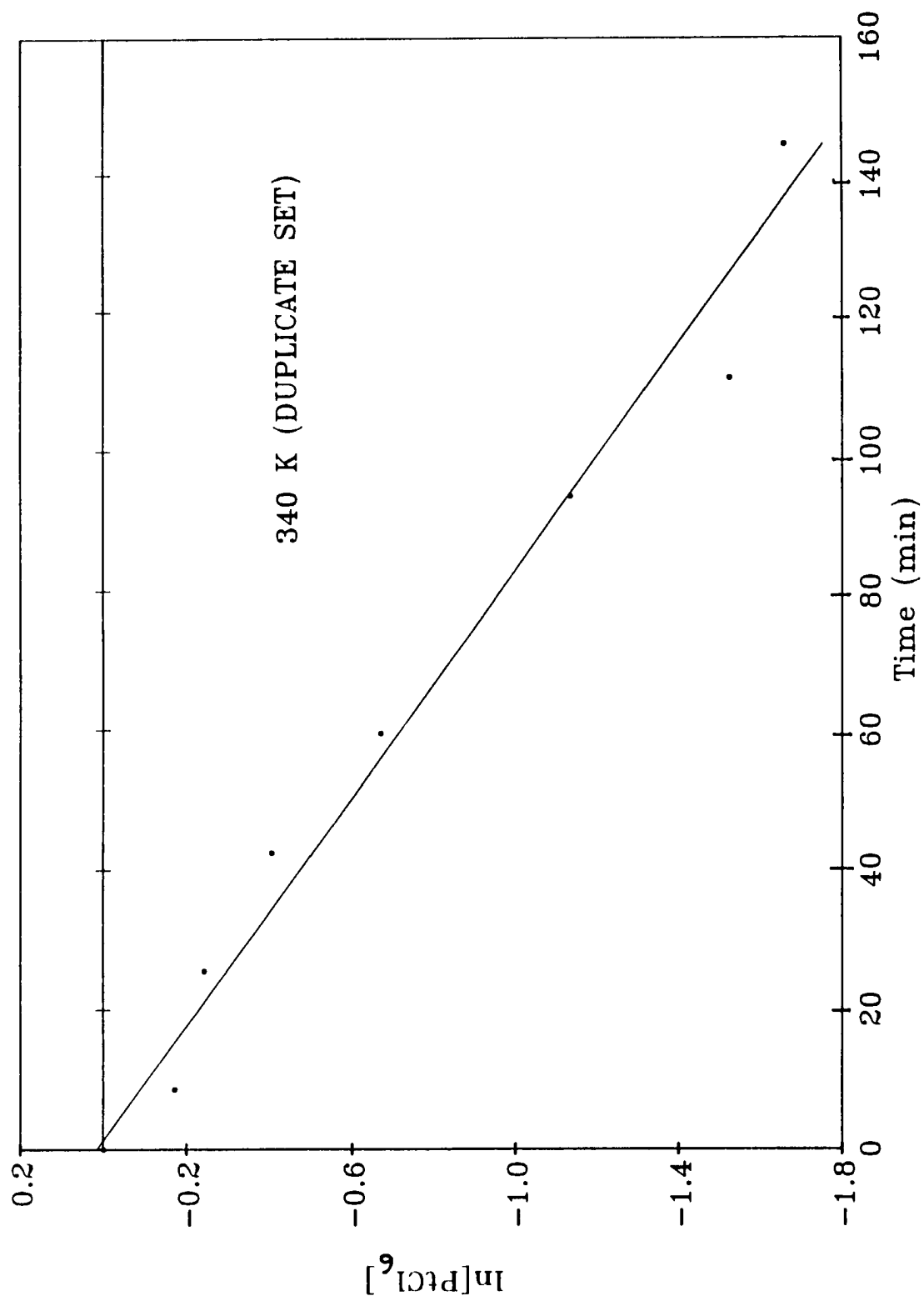




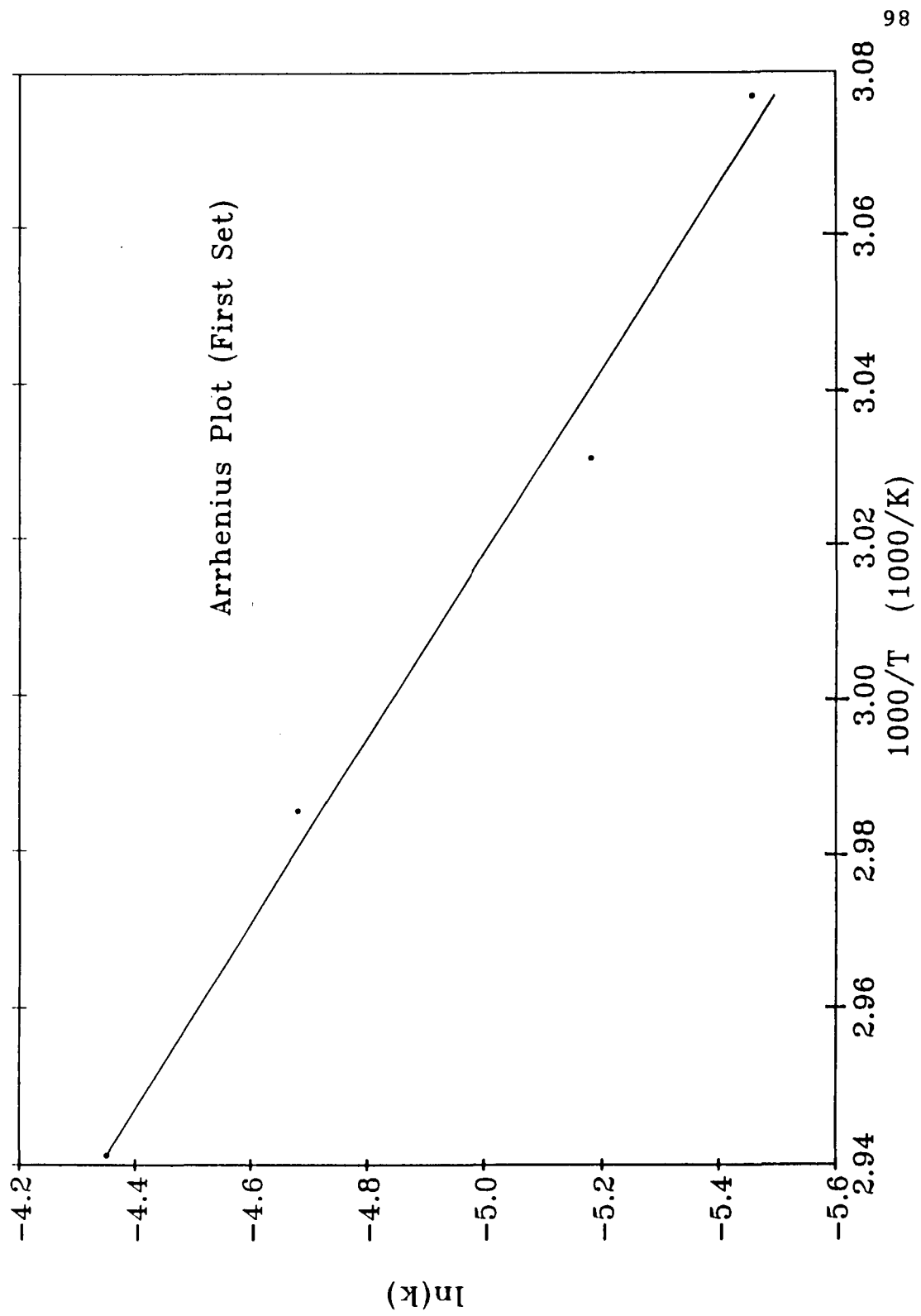


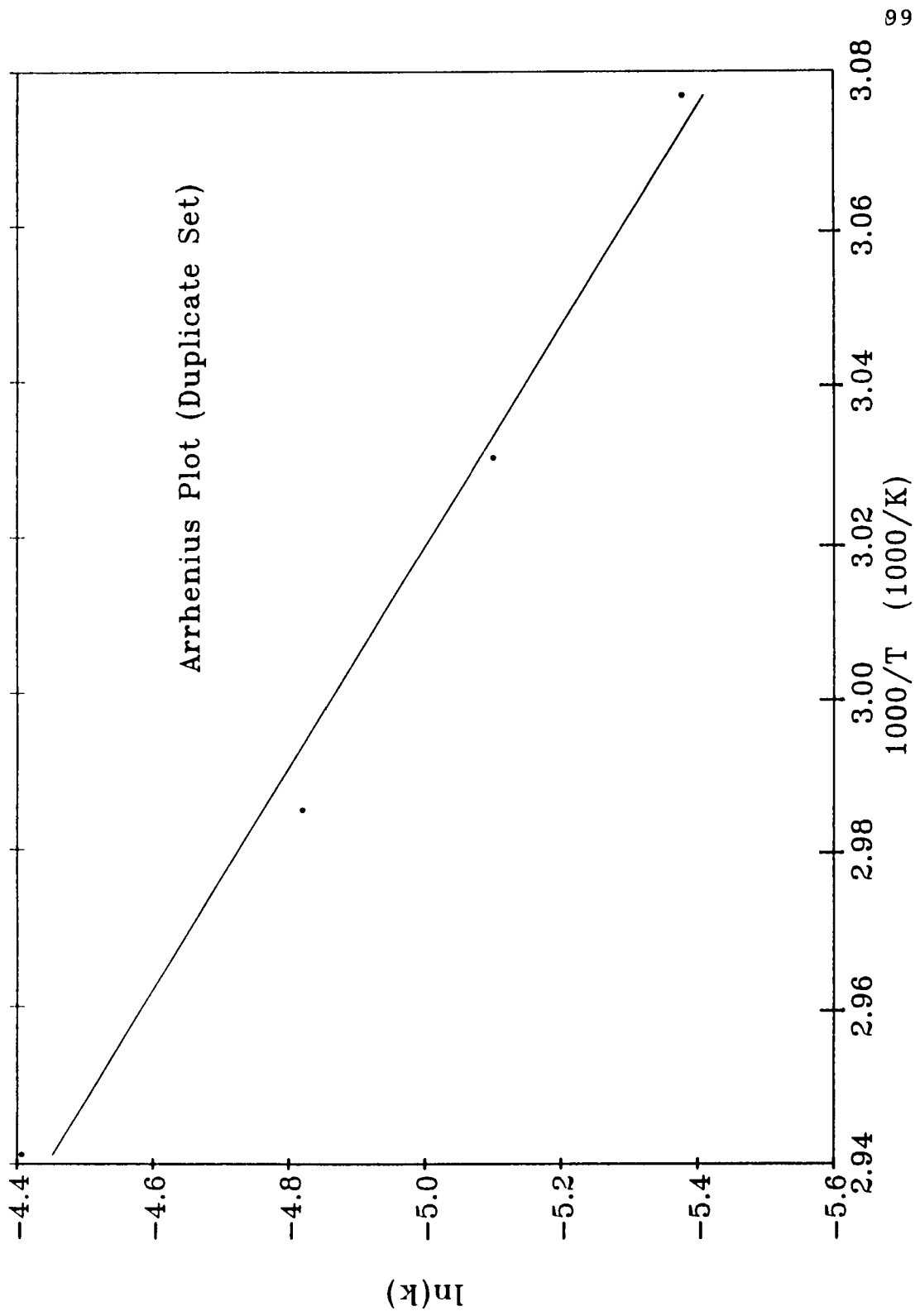




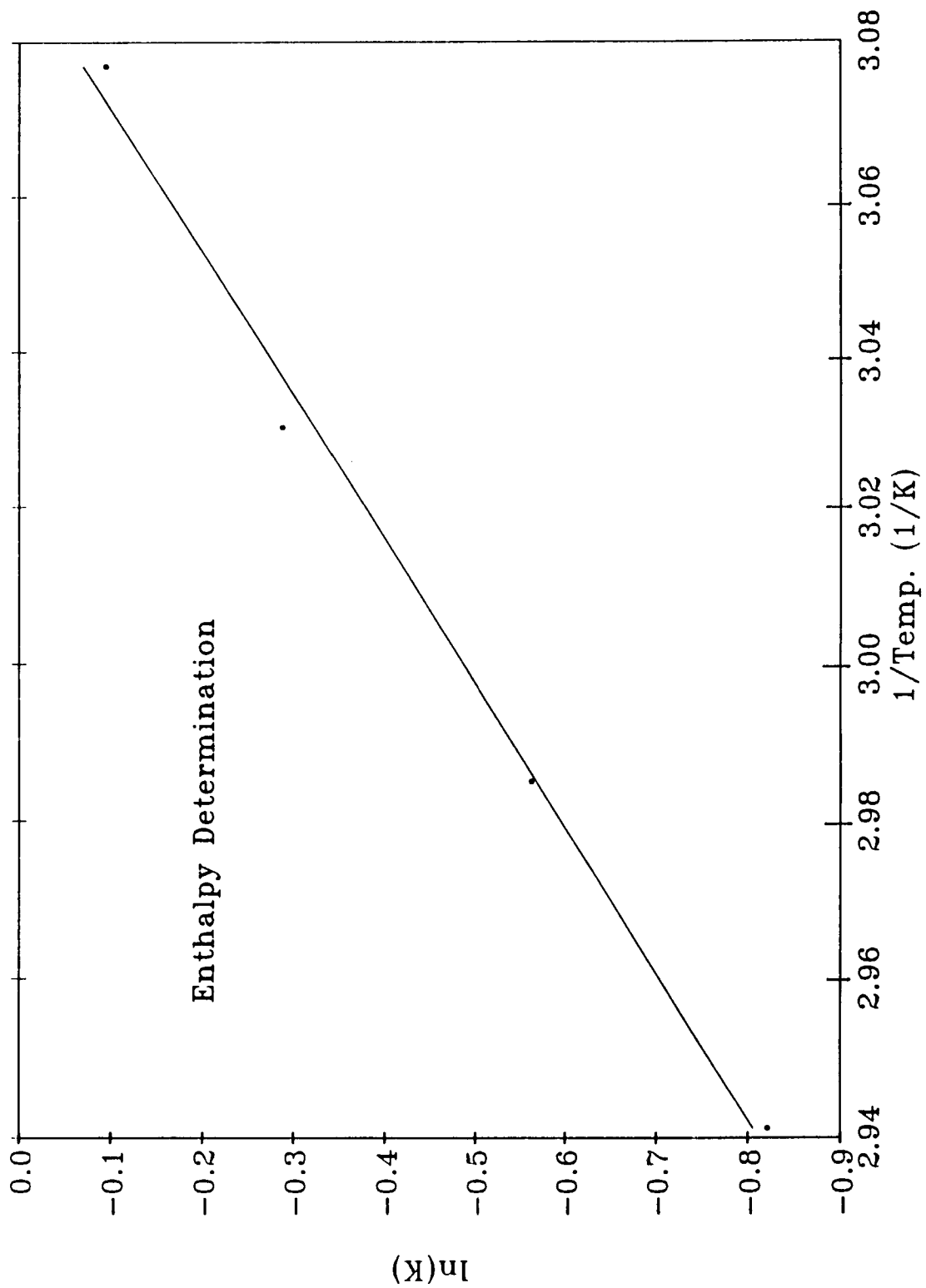


APPENDIX III





APPENDIX IV



LITERATURE CITED

LITERATURE CITED

1. Weast, R.C. Handbook of Chemistry and Physics, 63rd ed.; Chemical Rubber Company: Boca Raton, FL, **1982**, B-30.
2. Dobrota, M. Methodol. Surv. Biochem. Anal. **1987**, 17, 433.
3. Sakurai, H.; Tsuchiya, K.; Hirai, S.; Okada, Y.; Haraguchi, H. Naturwissenschcaften **1988**, 75(8), 405.
4. Uozomi, J; Litterst, C.L. J. Pharmacabio-Dyn. **1988**, 11(4), 277.
5. Reily, M.D.; Marzilli, L.G. J. Am. Chem. Soc. **1986**, 108, 6785.
6. Marcelis, A.T.M.; Erkelens, C; Reedijk, J. Inorg. Chim. Acta **1984**, 91, 129.
7. Haring, U.K.; Martin, R.B. Inorg. Chim. Acta **1982**, 78, 259.
8. Mansy, S.; Chu, G.Y.H.; Duncan, R.E.; Tobias, R.S. J. Am. Chem. Soc. **1978**, 100, 593.
9. Dijt, F.J.; Canters, G.W.; denHartog, J.H.J.; Marcelis, A.T.M.; Reedijk, J. J. Am. Chem. Soc. **1984**, 106, 3644.
10. Marcelis, A.T.M.; van Kralingen, C.G.; Reedijk, J. J. Inorg. Biochem. **1980**, 13, 213.
11. Cramer, R.E.; Dahlstrom, P.L. J. Am. Chem. Soc. **1979**, 101, 3679.
12. Marcelis, A.T.M.; Korte, H.J.; Krebs, B.; Reedijk, J. Inorg. Chem. **1982**, 21, 4059.
13. Jonson, R.; Mattson, S.; Unsgaard, B. Physics in Med. and Biol. **1988**, 33(7), 847.
14. Malinge, J.M.; Leng, M. Nucleic Acids Research **1988**, 16, 7663.
15. Krauss, M.; Basch, H.; Miller, K.J. Chem. Phys. Lett. **1988**, 148(6), 577.

16. Rahmouni, A.; Malinge, J.M.; Schwartz, A.; Leng, M. J. Biomolec. Struct. and Dyn. **1985**, 3(2), 363.
17. Sherman, S.E.; Lippard, S.J. Chem. Rev. **1987**, 87, 1153.
18. Kelley, S.L.; Basu, A.; Teicher, B.A.; Hacker, M.P.; Hamer, D.H.; Lazo, J.S. Science **1988**, 241, 1813.
19. Kuppen, P.J.K.; Schuitemaker, H.; Van't Veer, L.J.; DeBruin, E.A.; Van Oosterom, A.T.; Schier, P.I. Cancer Res. **1988**, 48(12), 3355.
20. Eastman, A.; Schulte, N. Biochemistry **1988**, 27, 4730.
21. Eastman, A. Biochemistry **1983**, 22, 3927.
22. Eastman, A. Biochemistry **1986**, 25, 3912.
23. Kuroda, R.; Ismail, M.I.; Sadler, P.J. J. Inorg. Biochem. **1984**, 22, 103.
24. Kuroda, R.; Neidle, S.; Ismail, I.M.; Sadler, P.J. Inorg. Chem. **1983**, 22, 3620.
25. Faggiani, R.; Lippert, B.; Lock, C.J.; Rosenberg, B. Canad. J. Chem. **1982**, 60, 529.
26. Erickson, L.E.; McDonald, J.W.; Howie, J.K.; Chow, R.P. J. Am. Chem. Soc. **1968**, 90, 6371.
27. Laszlo, P. NMR of Newly Accessible Nuclei; Academic Press: New York, **1983**; v.2.
28. Harris, R.K.; Mann, B.E. NMR and the Periodic Table; Academic Press, New York, **1978**.
29. Lycka, A.; Snobl, D.; Handlick, K.; Holecek, J.; Nadvorick, M. Collect. Czech. Chem. Commun. **1981**, 46, 245.
30. McFarlane, H.C.E.; McFarlane, W.; Turner, C.J. Mol. Phys. **1979**, 37, 1639.
31. Emsley, J.W.; Feeney, J.; Sutcliffe, L.H. High Resolution NMR Spectroscopy; Pergamon, Oxford, **1966**, v.2, 1082.
32. Kennedy, J.D.; McFarlane, W. Rev. Silicon, Germanium, Tin, Lead Compd. **1973**, 1, 235.
33. Pereyre, M.; Quintard, J.P.; Rahm, A. Pure Appl. Chim. **1982**, 54, 29.

34. Petrosyan, V.S. Progress in NMR Spectroscopy; Pergamon, Oxford, **1977**, v.11, 115.
35. Smith, P.J.; Smith, L. Inorg. Chim. Acta Rev. **1973**, 7, 11.
36. Smith, P.J.; Tupcianskas, A.P. Annual Report on NMR Spectroscopy; Academic Press, New York, **1978**, v.8, 292.
37. Armitage, I.M.; Otvos, J.D. Biological Magnetic Resonance; Plenum, New York, **1982**, v.4, 79.
38. Pregosin, P.S. Coord. Chem. Rev. **1982**, 44, 247.
39. Pesek, J.J.; Mason, W.R. J. Magn. Reson. **1977**, 25, 519.
40. Kerrison, S.J.; Sadler, P.J. J. Chem. Soc., Chem. Commun. **1977**, 861.
41. Freeman, W.; Pregosin, P.S.; Sze, S.N.; Venanzi, L.M. J. Magn. Reson. **1976**, 22, 473.
42. Kerrison, S.J.; Sadler, P.J. J. Magn. Reson. **1978**, 31, 321.
43. Anderson, S.J.; Goggin, P.L.; Goodfellow, R.J. J. Chem. Soc., Dalton Trans. **1976**, 1959.
44. Anderson, S.J.; Goodfellow, R.J. J. Chem. Soc., Dalton Trans. **1977**, 1683.
45. Galbraith, J.A.; Menzel, K.A.; Ratilla, E.; Kostic, N. Inorg. Chem. **1987**, 26, 2073.
46. Hallam, M.F.; Luke, M.A.; Mingos, M.P.; Williams, I.D. J. Organomet. Chem. **1987**, 325, 271.
47. Sebald, A.; Stader, C.; Wrackmeyer, B.; Bensch, W. J. Organomet. Chem. **1986**, 311, 233.
48. Al-Najjar, I.M. Inorg. Chim. Acta **1987**, 128, 93.
49. Appleton, T.G.; Hall, J.R. Inorg. Chem. **1971**, 10(8), 1717.
50. Appleton, T.G.; Berry, R.D.; Davis, C.A.; Hall, J.R.; Kimlin, H.A. Inorg. Chem. **1984**, 23, 3514.
51. Appleton, T.G.; Hall, J.R.; Ralph, S.F.; Thompson, C.S. Inorg. Chem. **1984**, 23, 3521.

52. Goggin; Goodfellow; Haddock; Taylor J. Chem. Soc., Dalton Trans. **1976**, 459.
53. Lopez, G.; Garcia, G.; Cutillas, N.; Ruiz, J. J. Organomet. Chem. **1983**, 241, 269.
54. Groning, O; Drakenberg, T.; Elding, L.I. Inorg. Chem. **1982**, 21, 1820.
55. Elding, L.I.; Groning, O. Inorg. Chem. **1978**, 17(7), 1872.
56. Carr, C.; Goggin, P.L.; Goodfellow, R. Inorg. Chim. Acta **1984**, 81, L25.
57. Drago, R.S. Physical Methods in Chemistry; Saunders: Philadelphia, **1977**; 188.
58. King, R.W.; Williams, K.R. J. Chem. Ed. **1989**, 66(9), A213.
59. Maskill, H. The Physical Basis of Organic Chemistry; Oxford University Press: New York, **1989**; 216.
60. McClave, J.T.; Benson, P.G. Statistics for Business and Economics; Dellen: San Francisco, **1988**; 556.
61. Adamson, A.W. Physical Chemistry; Academic Press: New York, **1979**; 227.
62. Marzilli, I.G.; Hayden, Y.; Reily, M.D. Inorg. Chem. **1986**, 25, 974.
63. McFarlane, W. J. Chem. Soc., Dalton Trans. **1974**, 324.
64. Dean, R.R.; Green, J.C. J. Chem. Soc. (A) **1968**, 3047.
65. Kennedy, J.D.; McFarlane, W. J. Chem. Soc., Dalton Trans. **1976**, 874.
66. Pidcock, A.; Richards, R.E.; Venanzi, L.M. J. Chem. Soc. (A) **1968**, 1970.
67. Rund, J.V.; Palocsay, F.A. Inorg. Chem. **1969**, 8(11), 2242.